

5-2017

Evaluating Amphibian Vulnerability to Mercury Pollution from Artisanal and Small-Scale Gold Mining in Madre de Dios, Peru

Kate Markham

Clark University, kmarkham@clarku.edu

Follow this and additional works at: https://commons.clarku.edu/idce_masters_papers

 Part of the [Environmental Studies Commons](#)

Recommended Citation

Markham, Kate, "Evaluating Amphibian Vulnerability to Mercury Pollution from Artisanal and Small-Scale Gold Mining in Madre de Dios, Peru" (2017). *International Development, Community and Environment (IDCE)*. 104.

https://commons.clarku.edu/idce_masters_papers/104

This Research Paper is brought to you for free and open access by the Master's Papers at Clark Digital Commons. It has been accepted for inclusion in International Development, Community and Environment (IDCE) by an authorized administrator of Clark Digital Commons. For more information, please contact mkrikonis@clarku.edu, jodolan@clarku.edu.

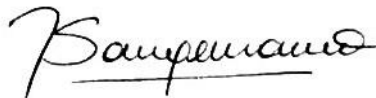
Evaluating Amphibian Vulnerability to Mercury Pollution from Artisanal and Small-Scale Gold Mining in Madre de Dios, Peru

Kate Markham
BSc, The George Washington University, 2011
MA, University of Victoria, 2014

May 2017

A Master's Research Paper submitted to the faculty of Clark University in Worcester,
Massachusetts in partial fulfillment of the requirements for the degree of Master of
Science in Environmental Science and Policy in the Department of International
Development, Community, and the Environment

And accepted on the recommendation of

A handwritten signature in black ink, appearing to read 'Florencia Sangermano', with a horizontal line underneath the name.

Dr. Florencia Sangermano

Abstract

Environmental hazards commonly associated with gold mining include local pollution of the air, water, and soil. Specifically, mercury used to extract gold bioaccumulates in the environment, contaminating rivers and watersheds and posing a danger to wildlife in regards to its developmental, hormonal, and neurological effects. To conceal these typically illegal operations happening along rivers, artisanal and small-scale gold mining (ASGM) often occurs in remote areas with high faunal biodiversity. The Madre de Dios region of southern Peru is a global biodiversity hotspot and has been undergoing extensive ASGM for years. The impact of ASGM on biodiversity is largely unknown. This study uses random forest classification to map mining area in Madre de Dios and models pollutant transport from ASGM sites to predict what locations and species assemblages at risk. Multi Criteria Evaluation is used to determine how flow accumulation, distance from mining area, total suspended sediment load, and soil porosity influence the vulnerability of regions to mercury pollution. The resulting risk map identifies areas of greatest risk of mercury pollution in Madre de Dios.

Acknowledgements

This paper would not have been possible without the tremendous support and expertise of my advisor, Dr. Florencia Sangermano. She supported my ideas, mentored me throughout this process, and taught me an incredible amount about remote sensing and conservation GIS. I only wish I could have stretched this degree out longer to learn more from her.

The time I spent in Puerto Maldonado and in Peru was invaluable as a researcher and significantly strengthened this paper. I am thankful for the incredible support I received from Amazon Conservation Association, the staff at Los Amigos Biological Station, particularly Carlos Quispe for helping me collect soil samples despite the rain and Renzo Piana for helping me arrive in Madre de Dios prepared to start my work. I owe many thank yous to all of the Peruvians who patiently answered my questions about mining and forest loss in Madre de Dios. I am very thankful to Antonio Fernandi for acting as a translator and providing lots of laughs.

I consider myself very lucky to have had considerable help and guidance from CINCIA while in the field and afterwards. Thank you to Julio Araujo and Francisco Roman for their wealth of knowledge and experience. Thank you also to Luis Fernandez for introducing me to CINCIA and for creating an organization with such a powerful mission.

Several professors at Clark provided advice and guidance throughout this paper whether in the classroom, or more often than not, outside of it including Drs. Sam Ratick, John Rogan, Denise Bebbington, Tony Bebbington, Fred Greenaway, Timothy Downs, Yelena Ogneva-Himmelberger, and Dale Hattis.

Lastly, I am thankful for the support of my friends and family, particularly my parents, for putting up with me and my crazy dream of becoming a researcher. I could not have done this without their laughter, advice, and patience. Thank you Will Thoman, Anam Khan, Laia Brugarolas Macia, Sam Upton, Ahna Miller, Bryan Buttigieg, Jason Ready, and Matt Zimmerman and many more in my IDCE cohort for always listening to me talk about mining.

This work would not have been possible without financial support from The George Perkins Marsh Institute and from the IDCE Department. I would have had a far less interesting and impactful project without visiting the field.

Introduction

The Madre de Dios region of southern Peru is one of the most biodiverse tropical regions on earth. The Amazon Rainforest, a World Wildlife Priority Place, covers much of the region. Multiple Important Bird and Biodiversity Areas (IBAs) and Evolutionarily Distinct and Globally Endangered (EDGE) species, such as the giant armadillo (*Prionomys maximus*), the lowland tapir (*Tapirus terrestris*), and the pygmy anteater (*Cyclopes didactylus*), are found there. Madre de Dios is home to some of Peru's most well-known protected areas, such as Manú National Park (a UNESCO Natural World Heritage Site and Conservation International Biodiversity Hotspot), Tambopata National Reserve, and Amarakaeri Communal Reserve. Manú National Park and surrounding buffer areas cover 0.1% of the earth's land but are home to 2.2% and 1.5% of world's amphibians and reptiles respectively, making it the top biodiversity hotspot in the world for these animals (Catenazzi et al., 2013).

Biodiversity in Madre de Dios is threatened by resource extraction, particularly gold mining. Peru is currently the world's sixth largest producer of gold (USGS, 2015). The increase in the price of gold since the latest economic downturn (Shafiee and Topal, 2010) has made it profitable to mine from previously unprofitable areas, such as deposits below tropical forests (Swenson et al., 2011). In many instances, mining in tropical forests occurs in or close to protected areas of high biodiversity (Alvarez-Berrios and Aide, 2015). In Peru, illegal gold mining has already been reported in Tambopata National Reserve (Finer et al., 2015; 2016).

From 1999 to 2012, Madre de Dios lost 500 km² of forest due to gold mining (Asner et al., 2013). Artisanal and small-scale mining (ASM) is typically conducted informally by local miners for subsistence or for a small business. ASM is done with little mechanization, relying instead mainly on manual labor. In Peru, small-scale and artisanal mining is defined as concession areas of up to 2,000 and 1,000 hectares and production of up to 350 and 25 metric tons respectively (MINEM, 2002). ASM is often ignored in calculations of forest loss due to methodological difficulties, yet when ASM activities are included in estimates of deforestation, the amount of forest lost increases substantially (Asner et al., 2013). Since 2007, the primary contributor to land change in the Southwest Amazon region in Peru has been artisanal and small-scale gold mining (Scullion et al., 2014). The average rate of forest loss due to gold mining tripled from 1999-2007 to 2008-2012 (Asner et al., 2013).

Environmental threats associated with mining extend beyond deforestation. Arsenic, cyanide and mercury (Hg) pollution of the air, water, and soil are commonly associated with mining (Eisler and Wiemeyer, 2004; Veiga et al., 2006). Liquid Hg used to amalgamate and concentrate metals, including gold, is released into the atmosphere during burning, and enters the environment through tailings or mining byproducts. On average, ASM mining is significantly dirtier per unit of output when compared to other types of mining (McMahon et al., 1999).

Methylmercury (MeHg) forms when elemental Hg is methylated by aquatic organisms and bacteria. Uncharged complexes of Hg are taken up by bacteria with production of MeHg more likely to occur when pH is low (Jensen and Jernelov, 1969; Beijer and Jernelov; Fagerstrom and Jernelov). MeHg is the most toxic organic form of Hg and bioaccumulates and biomagnifies through the aquatic food chain (Baeyens et al., 2003; Fitzgerald and Clarkson, 1991; Mason et al., 2006).

Amphibians may be particularly at risk to Hg contamination given their current global decline and extinction (Stuart et al., 2004) and their dependence on water during the larval stage. Mercury pollution has been related to decrease in food consumption, size and mortality rate of amphibians. Two-lined salamanders (*Eurycea bislineata*) collected at sites with high Hg levels consume half as much as salamanders collected at uncontaminated sites and appear to have slower responses and speed (Burke et al., 2010). American toads (*Bufo americanus*) exposed to Hg through maternal transfer or through their diet as larvae are 7% smaller than control subjects, indicating Hg effects persist after metamorphosis (Todd et al., 2012). *B. americanus* larvae exposed to Hg through maternal transfer and diet experience 50% higher mortality than controls (Bergeron et al., 2011). Previous work in Madre de Dios has determined that Hg levels in water and soil are elevated in areas downstream of artisanal and small-scale mines (Diringer et al., 2015) and Hg levels in raptors are elevated (Shrum, 2009), so it is reasonable expect amphibians in this region are presently at risk.

While previous research has used remotely sensed data to identify mining areas in Madre de Dios (Elmes et al., 2014; Asner et al., 2013), this project is the first to use random forest classification to map ASGM activity and to create a model identifying areas likely polluted with mercury. Deforestation due to mining is presently being mapped by researchers at the Monitoring of the Andean Amazon Project, but the distribution of Hg in the region remains largely unstudied. Models of mercury transport in aquatic environments where remote sensing and GIS techniques have contributed significantly to the study have been created for south-western China (Lin et al., 2011) and South Carolina (Knightes et al., 2014). This current study uses remotely sensed data and multi criteria assessment to expand on existing knowledge of ASGM activities in Madre de Dios by studying amphibian vulnerability and determining where wildlife in general may be threatened by Hg pollution.

To date, there is a dearth of research on wildlife and biodiversity surrounding active and inactive ASGM areas. This study maps the area vulnerability to Hg pollution and relates it to protected reserves, national parks and areas of high amphibian biodiversity.

We seek to answer the following questions: how has ASGM changed the landscape of Madre de Dios; what areas are at greatest risk to mercury pollution; and where might amphibian biodiversity in Madre de Dios be affected by mercury pollution?

By studying the effects of gold mining on biodiversity in one of the most biodiverse areas on the planet, this research will identify areas where formal protection should be evaluated or existing protected areas should be expanded. Identifying areas of low amphibian biodiversity and low vulnerability may also allow natural resource managers and Peruvian officials to minimize environmental impact when future mining concessions are being created or future mining permits are released.

Methods

Data sources

Table 1. Data sources, resolution, and their usage in the study

Data	Used for	Source	Resolution
USGS Landsat data	RF classification	USGS	30m
DEM	Flow accumulation and friction layer for cost distance from mining area	ASTER	1 arc-second or 30m
Protected Areas		IRENA	N/A
Amphibian Biodiversity		BiodiversityMapping.org	10km
Bulk density at 2.5cm depth	Soil porosity	SoilGrids1km	250m

Study region

The study region is a select portion of the Madre de Dios region of Peru (Fig 1). This includes the Madre de Dios, Colorado, Inambari, and Malinowski rivers as well as a portion of the Andes. Manu National Park lies to the west of the Colorado River on the other sides of the Amarakaeri Communal Reserve. Tambopata National Reserve and Bahuaja Sonene National Park are in the southeast portion of the study region. The city of Puerto Maldonado is included and the Huepetuhe and Guacamayo mining areas. As of 2011, the Peruvian Ministry of the Environment estimated that more than 32,000 hectares of forest had been destroyed by mining activity.

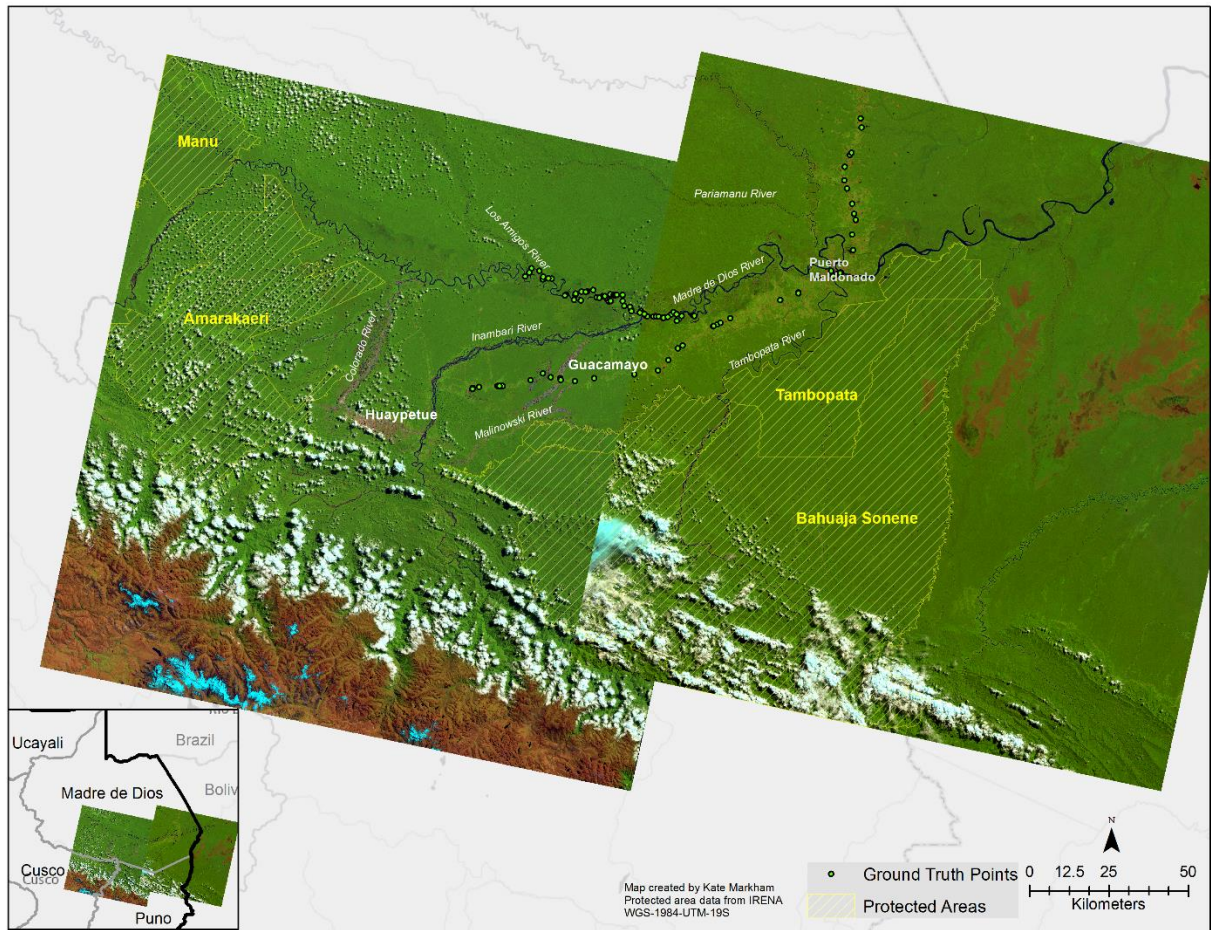


Figure 1-False color composite of study region. Protected areas overlaid in yellow. Ground truth points in green. The city of Puerto Maldonado is shown as well as the major mining areas of Huaypetue and Guacamayo.

This study first created land classification maps using random forest classification to identify mining areas in the study region. Multi Criteria Evaluation (MCE) using Ordered Weighted Averaging (OWA) was then used to map the vulnerability to Hg pollution based on environmental and chemical factors. Methods are divided in four parts: 1) the land cover classification, 2) land change analysis 3) Hg vulnerability modeling, and 4) biodiversity assessment.

1) Land cover classification and change modeling

A land-cover map for the Madre de Dios region was created based on a supervised classification of Landsat ETM+ and OLI scenes (Table 2). Scenes were atmospherically corrected using the Cos (T) method and clouds were masked using thresholds identified from spectral mixture analysis.

Table 2. Data Used for Random Forest Classification

Date	Row/ Column	Landsat	Iron Oxide Indices	Composite and Training Sites
2015- Aug 29	3/69	8 OLI	b4/2 and b4/3	Bands 1-7, iron indices, bright green wet measurements Training sites: forest, vegetation, bare soil, sand, mining sediment, water type I, water type II, shadow
2015- Sept 7	2/69	8 OLI	b4/2 and b4/3	Bands 1-7, iron indices, bright green wet Training sites: forest, vegetation, bare soil, sand, mining sediment, water type I, water type II, shadow
2001- Aug 30	3/69	7 ETM+	b3/1 and 3/2	Bands 1-5,7 iron indices, bright green wet Training sites: forest, vegetation, bare soil, sand, mining, water, shadow
2001- Aug 23	2/69	7 ETM+	b3/1 and 3/2	Bands 1-5,7 iron indices, bright green wet Training sites: forest, vegetation, bare soil, sand, water type I, water type II, shadow <i>*note mining was not apparent in the 2001 2/69 tile and thus was not included as a class</i>

Random Forest classification was used to determine land cover classes (randomForest package in R, Liaw and Wiener, 2002). This supervised classification method uses multiple classification trees. Trees are trained on a sample of training data; the algorithm determines the split at each node by searching a random subset of variables using bootstrap aggregating of training data. At each node of the tree, the data is split until a terminal node or leaf is reached. With each split, the nodes become increasingly pure.

Random forest is a type of machine learning that uses ensembles of classifications, resulting in greater accuracy compared to other machine learning techniques. Increased accuracy arises from the use of multiple classifiers, relying on the strengths of said classifiers while avoiding weaker classifiers (Ghimire et al., 2010; Kotsiantis and Pintelas, 2004). It has been shown that random forest increase land cover classification accuracy when compared to support vector machines (Pal, 2005). The advantages of Random Forest are that it produces a large number of trees, reducing generalization error and overfitting, it estimates which variables are important to classification, and it is robust to outliers and noise (Breiman, 2001).

First, spectral training sites for: forest, vegetation (non-forest), bare soil, sand, mining sediment, water (two types used in some classifications with distinct spectral signatures), and shadow were digitized in Terrset (Eastman 2016). Two thousand training samples were selected for each land cover class. Classification was performed on a combination of indices selected for their capability to identify iron oxide, soil, vegetation and moisture. Two iron oxide indices (Warner and Campagna, 2013) were used to differentiate sand and bare soil from mining areas. These indices have been

used previously to map gold mining areas (Gabr et al., 2010; Pour and Hashim, 2015). Measures of brightness (indicative of soils), greenness, and wetness/moistness were extracted from a Tassel Cap Transformation using a Kauth and Thomas 4-dimensional transformation on six bands to produce three new index bands (Kauth and Thomas, 1976; Haung et al., 2002; Baig et al., 2014). Spectral signatures of the training sites used for each classification can be found in Appendix I.

Class error rates for each of the random forest classification land cover classes were less than 0.01% in all instances. The resulting output was examined and necessary edits for obvious errors (clouds identified as mining area for example) were made.

A Mahalanobis typicality classification was also run using the same training sites. The results were compared with the random forest classification and areas identified as mining by both classifications were used as the inputs for the generation of factors to be used in the vulnerability modeling. A classification threshold of 75% was used for random forest and a 40% threshold for Mahalanobis such that any pixel that did not meet the aforementioned thresholds remained unclassified.

The random forest land cover classification was validated by collecting ground truth locations from 106 points located along the Interoceanic Highway and along the Madre de Dios River by boat in June and July of 2016. Locations were chosen based on their accessibility. Due to accessibility restrictions, imagery from Google Earth for corresponding dates were used to complement the accuracy assessment. Points per land class were randomly generated using stratified random sampling. The area validated for accuracy was restricted by a 5km buffer surrounding rivers, given that mining activity require moving water to operate.

2) Land change modeling

The Land Change Modeler (LCM) in Terrset (Eastman, 2009) was used to identify changes from land cover types from 2001 to 2015. LCM generates maps showing the transition from one cover type to another and calculates net change, contributors to change, and gains and losses by land cover type. The land cover classification produced from Random Forest was used.

3) Hg vulnerability modeling

MCE allows the generation of vulnerability to Hg by combining the contribution to Hg vulnerability from multiple environmental and chemical factors. Factors likely to influence the vulnerability of an area to Hg pollution were selected and weighted based on literature review.

A model was done independently for land and river areas, with vulnerability factors selected based on availability of data and relevance (Lin et al., 2011; Ullrich et al., 2010). The factors included for river vulnerability were: 1) distance from mining area; 2)

average suspended sediment of river; 3) flow accumulation and; 4) mean estimate of sediment porosity at the 22.5cm layer depth (Fig 2). For land vulnerability, factor 2 did not apply, and flow accumulation was replaced with an inverse of elevation to account for low-lying areas on land.

In a multi- criteria evaluation factors are weighted based on their contribution to Hg vulnerability, and then aggregated to result in the final Hg vulnerability map. Aggregation can have different levels of risk and tradeoff and these levels can be controlled by calculating Ordered-Weighted-Averages (OWA). OWA allows to determine how pessimistic/optimistic or risk-averse/risky the model is in determining trade-off between factors. This is accomplished through using an ORness value. A greater ORness value means that high values in one factor cannot be averaged out by low values in another factor. Higher ORness values reduce the likelihood of Type II errors.

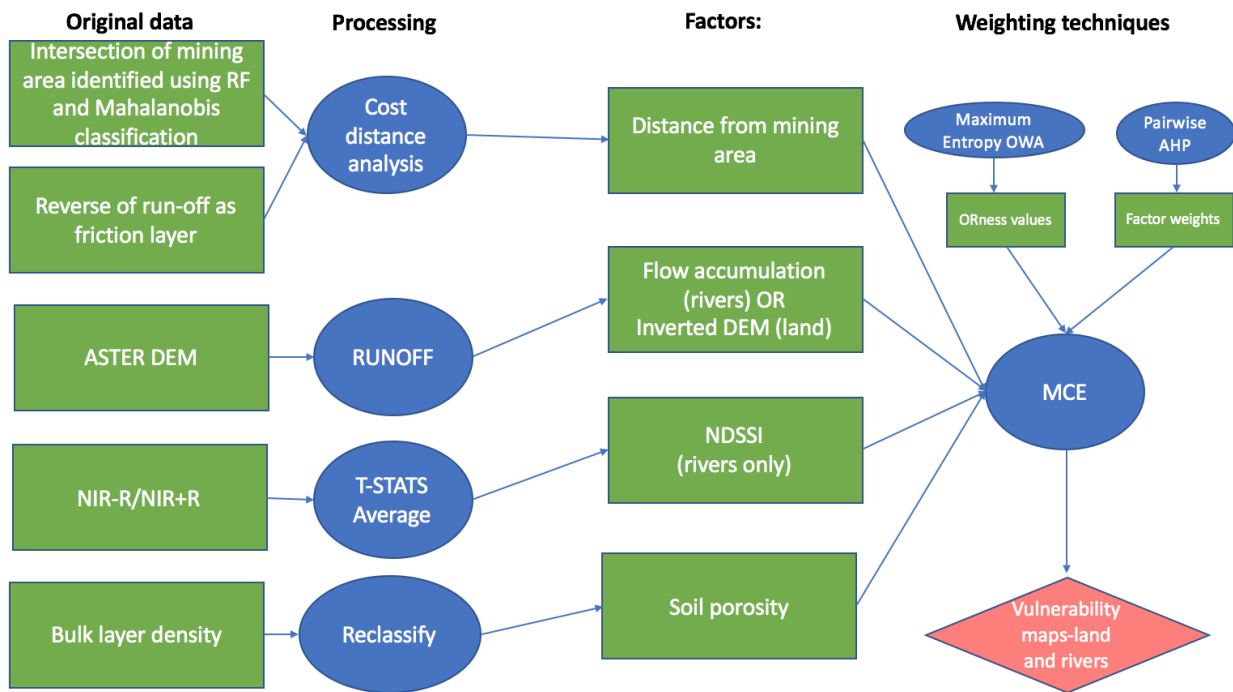


Figure 2 Flow diagram of methods used to generate vulnerability map

Distance to mining areas was generated by using a cost distance approach which determines the minimum cost from each cell to the nearest source using a friction layer. In this study, mining area acted as the source and slope generated from ASTER DEM data was used for the friction layer with greater slopes providing greater resistance to distance traveled.

Flow accumulation was generated through a run-off model from ASTER DEM at 30m resolution data in Terrset (Eastman, 2016). Runoff processes simulate where Hg is transported and are used as an important input in related studies modeling pollutant

transport (Lin et al., 2011; Kheir et al., 2014). When modeling land vulnerability, the inverse of DEM data was used to account for lower elevations having increased susceptibility to Hg carried downslope by gravity.

Since most mercury in water is bound to sediments (Andren and Harriss, 1975; Mason and Benoit, 2003; Cossa et al., 1994; Mason et al., 1993), an average normalized difference suspended sediment index (NDSSI) was used as a factor. This factor was created by averaging NDSSI indices created for six Landsat scenes taken between the months of July and October for the years of 2013-2016. Selected scenes had less than 20% cloud coverage, and the NDSSI was created following the work of Azad Hossain, Chao, and Jia's (2010), where $NDSSI = \frac{NIR-Red}{NIR+Red}$. Post cloud-masking, only pixels for which there were a minimum of three data values were included in the index calculation. As much as 95% of total Hg is bound to suspended particles (Hines et al., 2000; Horvat et al., 2003; Zhang et al., 2010).

Sediment porosity was calculated from the World Soil Information's SoilGrids1km (Hengl et al., 2017 through ISRIC-WDC Soils) data at 250m resolution by inverting mean estimates of bulk soil density at the 22.5cm depth. Soil characteristics such as soil porosity are used in related studies modeling pollutant transport or land suitability analysis (Kheir et al., 2014; Bagdavičiūtė and Valiūnas, 2013). Bagdavičiūtė and Valiūnas (2013) incorporate soil permeability but, because groundwater pollution is considered, higher soil permeability increases vulnerability in this study. Because we are concerned with amphibians that are exposed to pollutants transferred through their permeable skins, it is reasoned that lower soil permeability increases the amount of Hg present at the surface level and thus the contact with amphibians.

All factors were standardized to a scale of 0-100 using a linear stretch that rescaled the values between the minimum and maximum values.

Importance weighting

Factor weights were determined using a pairwise Analytical Hierarchy Process (AHP), using the principle eigenvector of the pairwise comparison matrix. The resulting weights sum to 1 and follow the logic of Saaty (1997). Factors used for modeling land vulnerability included cost distance from mining area, inverted DEM, and soil porosity (Table 3). Factors used for modeling river vulnerability included cost distance from mining area, runoff, NDSSI, and soil porosity (Table 4). The consistency ratio for both set of factors was acceptable (0.06 in both cases).

Table 3. Factors used in modeling land vulnerability with weights and explanation of effect on vulnerability

Factor	Explanation	Weight
Distance from mining area	Cost distance from area classified as mining. ↓ distance=↑vulnerability	.6491

Digital Elevation Model (DEM)	Elevation inverted. ↓ elevation=↑vulnerability	.2790
Soil porosity	↑soil permeability=↑ vulnerability	.0719

Table 4. Factors used in modeling river vulnerability with weights and explanation of effect on vulnerability

Factor	Explanation	Weight
Distance from mining area	Cost distance from area classified as mining. ↓ distance=↑ vulnerability	.5660
Runoff	Calculated surface runoff. ↑ runoff=↑ vulnerability	.2674
Mean suspended sediment (NDSSI)	Average suspended sediment index. ↑ suspended sediment=↑ vulnerability	.1267
Soil porosity	↑soil permeability=↑ vulnerability	.0399

Ordered weighted averaging MCE

Models were run with ORness levels 0, 0.25, 0.5 (a weighted linear combination), 0.75, and 1.0 for both land and rivers. A non-linear model (Fig 3) was used to determine weights that maximize entropy while observing the pre-determined ORness (Malczewski et al., 2003). The resulting weights for each ORness level are shown in Tables 5 and 6.

Table 5. Weights given to each factor based on ORness value used to model land vulnerability

ORness	1 st ranking (minimum)	2 nd ranking	3 rd ranking (maximum)
0	1	0	0
0.25	0.4662	0.3175	.2162
0.5	0.33	0.33	0.33
0.75	0.2162	0.3175	0.4662
1	0	0	1

Table 6. Weights given to each factor based on ORness value used to model river vulnerability

ORness	1 st ranking (minimum)	2 nd ranking	3 rd ranking	4 th ranking (maximum)
0	1	0	0	0
0.25	0.5258	0.2680	0.1366	0.0696
0.5	0.25	0.25	0.25	0.25
0.75	0.0696	0.1366	0.2680	0.5258
1	0	0	0	1

Maximize $E(W) = -\sum_{i=1}^n w_i \ln w_i$ [Maximum Entropy OWA]

Subject to $\alpha = \frac{1}{n-1} \sum_{i=1}^n (n-i)w_i$ ($\alpha = orness$)

$w_i \in [0, 1], i = 1, \dots, n$

Figure 3 Equation used for Maximum Entropy Ordered Weighted Analysis

Vulnerability is sensitive to the weights given to each factor and to the ORness values that determine trade-off between factors. The sensitivity of the model to ORness values was determined by calculating the standard deviation for all five models run for both land and rivers.

4) Biodiversity risk assessment

Shapefiles of protected areas were obtained from the Peruvian National Institute of Natural Resources (IRENA). Amphibian biodiversity at 10 km resolution was obtained from BiodiversityMapping.org which uses species range maps from IUCN to create species richness maps in raster format (Fig 4).

To determine which areas are most at risk in relation to amphibian species richness, a prioritization of each 10 km pixel was completed using irreplaceability-vulnerability plots (Margules and Pressey 2000). Such irreplaceability-vulnerability maps have been used previously to inform and prioritize protection (Noss et al., 2002; Linke et al., 2007; Sangermano et al., 2012). To create such a plot, species richness (x-axis) was plotted against vulnerability (y-axis) at the pixel level and divided into quadrats. The upper, right-hand most quadrat of the plot shows the pixels with the highest species richness and highest vulnerability.

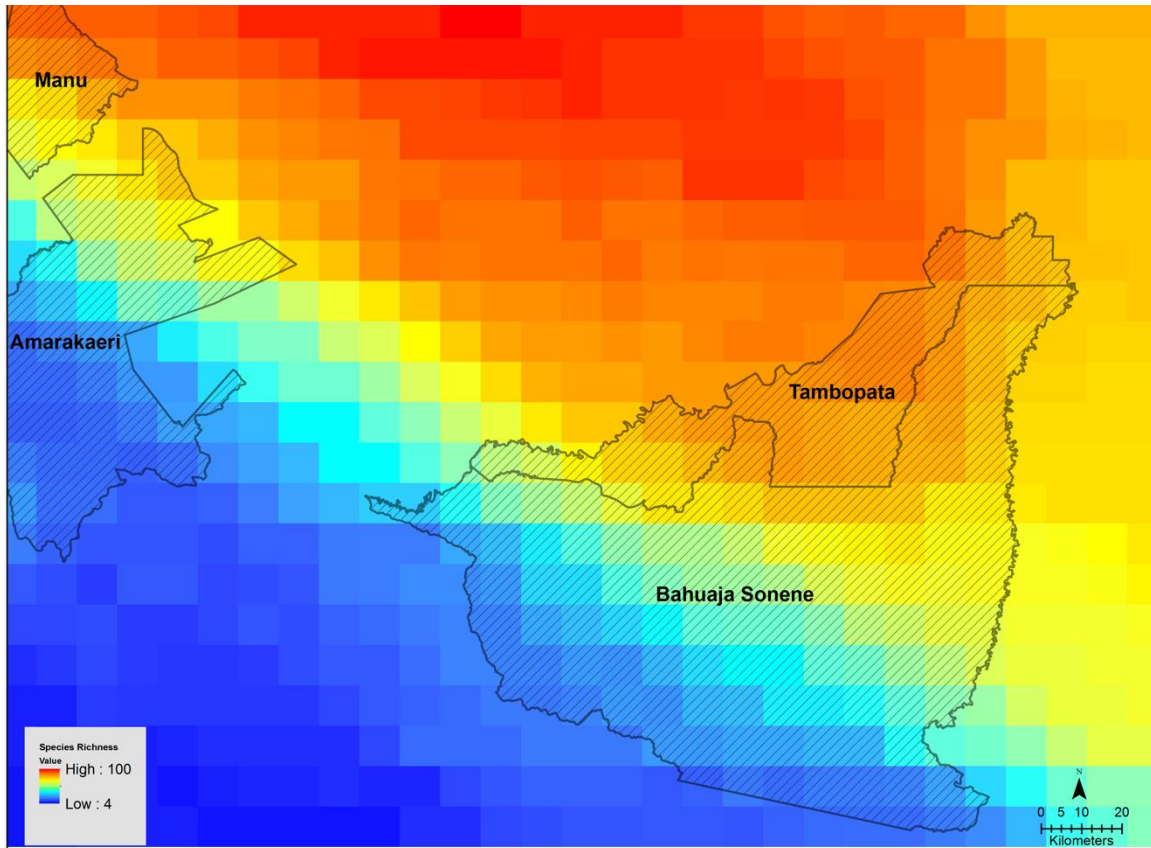


Figure 4 Amphibian biodiversity, as measured by species richness, in Madre de Dios at 10km resolution. Protected areas outlined in black.

Results

Madre de Dios landscape change due to ASGM

Visual inspection of the random forest outputs with no threshold set for classification show the Huaypetue and Guacamayo mining areas are visible and successfully classified as mining in the 2015 satellite images (Fig 5). Mining is also present along the Madre de Dios River. In 2001, the Guacamayo mining area did not exist and the Huaypetue mining area is largely classified as sand although some of the sediment in this region is classified as mining (Fig 6).

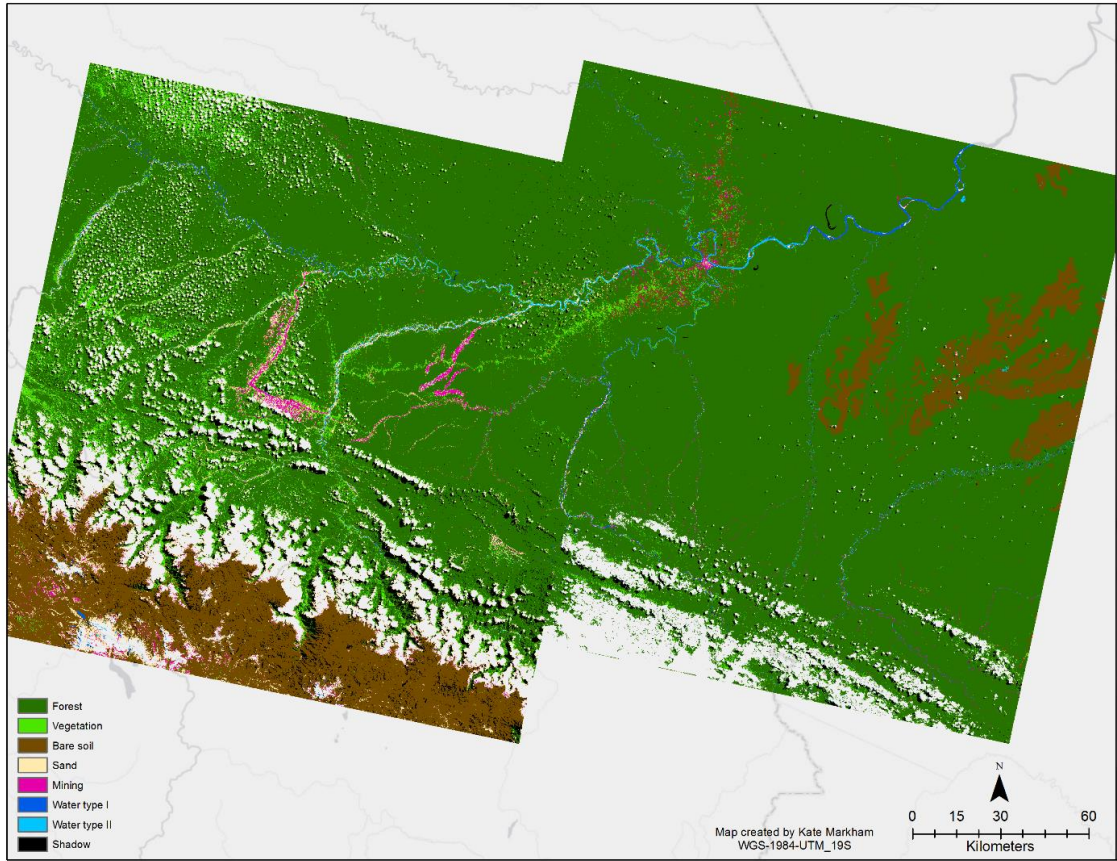


Figure 5 Results of random forest classification for 2015

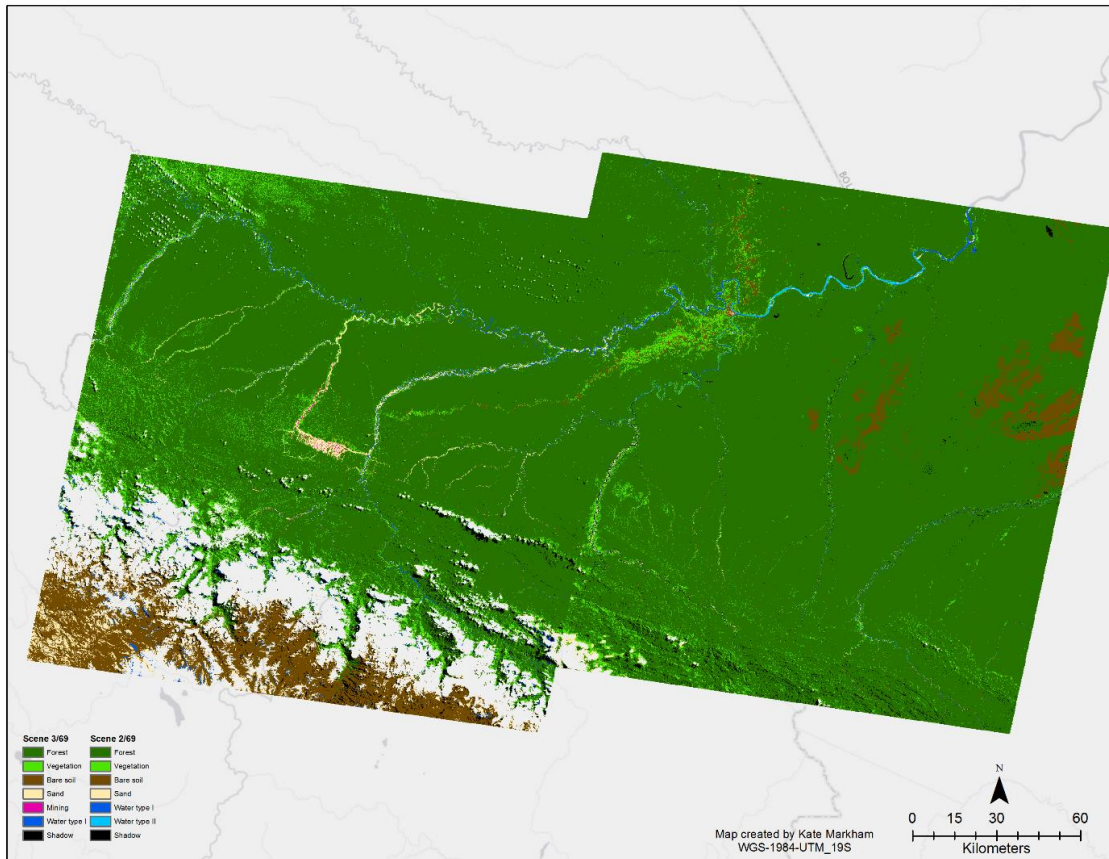


Figure 6 Results of random forest classification from 2001

Since 2001, the study region has gained 115.97km² of mining area (Table 5). Mining area made up less than 0.01% of the study area in 2001. In 2015, this percentage had increased to 2%. Forest coverage dropped from roughly 20,500 km² to less than 18,000 km² in 2015.

Table 5. Changes in land cover from 2001 to 2015 (note, percentages will not sum to 100 because water and misclassified areas are excluded).

Land cover type	2001 area km ²	2001 area %	2015 area km ²	2015 area %	% change
Forest	20487.06	84	17788.16	79	-5
Vegetation	3125.82	5	2773.61	5	0
Bare soil	3727.43	6	7132.35	12	6
Sand	1082.03	<2	1697.86	3	1
Mining	5.84	<0.01	121.65	2	2

Land cover types that contributed to the gain in mining area include forest, sand, vegetation, and bare soil. Of the 115.97 km² the mining land cover type gained, 64.86 km² was from forested area, 32.90 km² from sand, and 8.66 km² from non-forest

vegetation. Changes to land cover from 2001 to 2015 due to mining are shown in Figure 7.

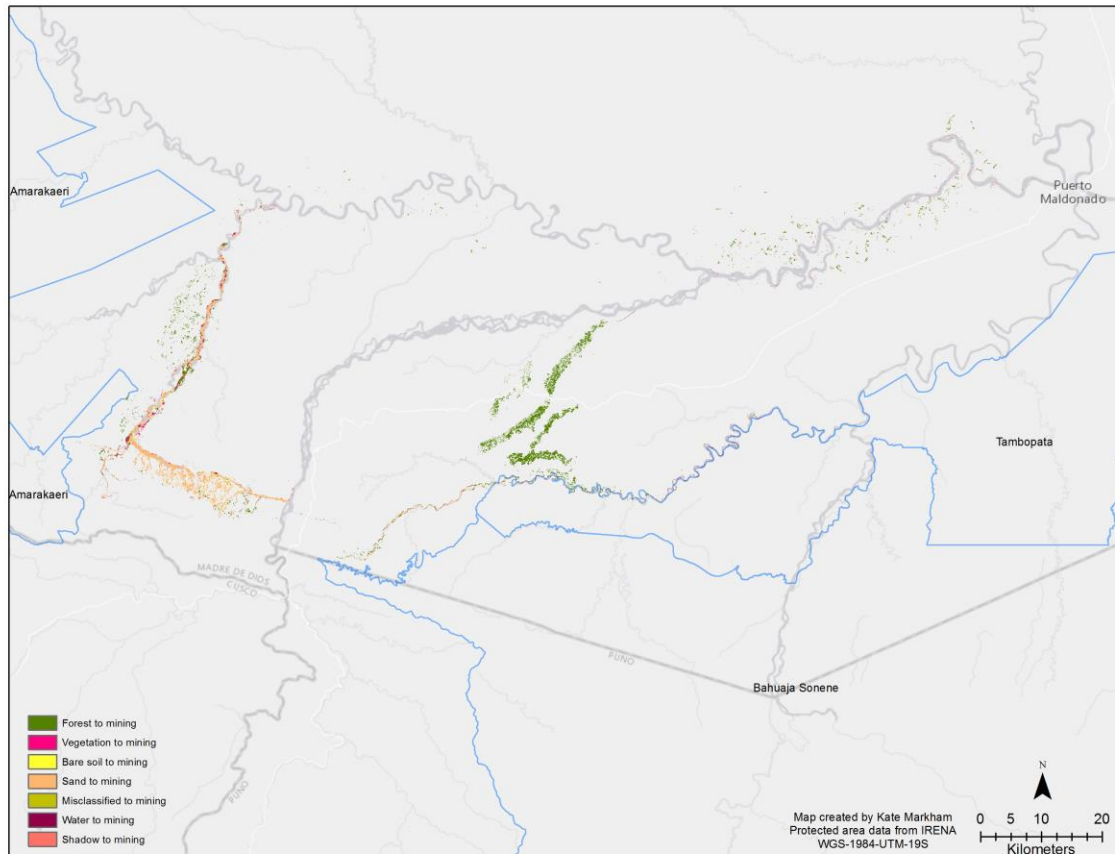


Figure 7 Mining-related changes to land cover from 2001 to 2015. Protected areas outlined in blue. The city of Puerto Maldonado is identified in the upper right hand corner of the map.

Accuracy assessment using Google Earth imagery omission error rate of 0.2 with no commission errors. The spectral class closest to mining, sand, was never classified as mining nor was mining ever classed as sand (Table 6).

Table 6. Error matrix for land classes of 2015 image using Google Earth Imagery

	Forest (Predicted)	Vegetation	Bare soil	Sand	Water	Mine	Omission error
Forest (Actual)	39	0	0	0	0	0	0
Vegetation	5	5	0	0	0	0	0.5
Bare soil	0	2	8	0	0	0	0.2
Sand	6	0	0	4	0	0	0.6
Water	0	0	0	0	10	0	1
Mine	0	0	0	0	2	8	0.2
Commission error	0.22	0.29	1	1	0.17	1	-

Accuracy assessment using only visited ground truth locations proved lower accuracy than using Google Earth imagery (Table 7). Errors of omission for mining were higher increasing from 0.2 to 0.65.

Table 7. Error matrix for land classes of 2015 image using ground truth locations

	Forest (Predicted)	Vegetation	Bare Soil	Sand	Water	Mine	Misclassified	Omission Error
Forest (Actual)	-	-	-	-	-	-	-	-
Vegetation	2	14	5	0	0	0	0	0.67
Bare Soil	0	3	7	0	0	0	0	0.70
Sand	1	1		13	0	0	3	0.72
Water	0	0	0	0	2	0	0	1.00
Mine	0	0	2	7	0	16	21	0.35
Commission Error	-	0.78	0.5	0.7	1	1	-	-

Areas at high risk to mercury pollution

Areas of high vulnerability vary depending on the ORness level chosen, with some areas varying by as much as 40 points in their vulnerability index value (Fig 8).

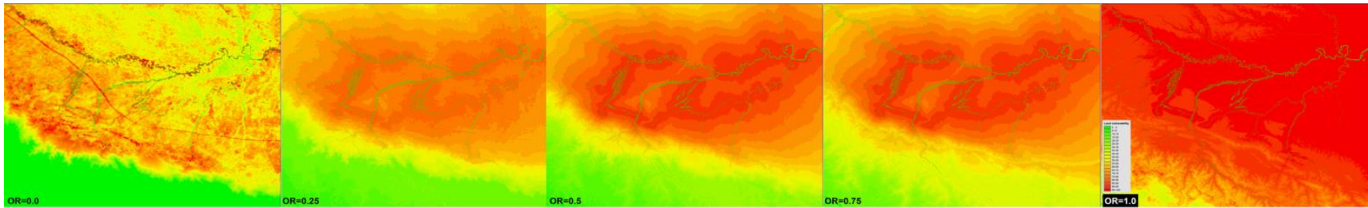


Figure 8 Range of land vulnerability dependent on ORness value ORness values increase from left to right. Vulnerability increases from green to red.

On average, 19,576km² of land have a vulnerability of 70 or higher (Fig 9). Vulnerable areas extend into Tambopata National Reserve, Bahuaja-Sonene National Park, and AmaraKaeri Communal Reserve (Fig 9). Areas within Manu National Park is presently considered to be at low risk. There are also scattered areas of high risk along the Madre de Dios River in the northern portion of the study area. This includes a scientific research station, Los Amigos Biological Reserve, and its conservation concession area.

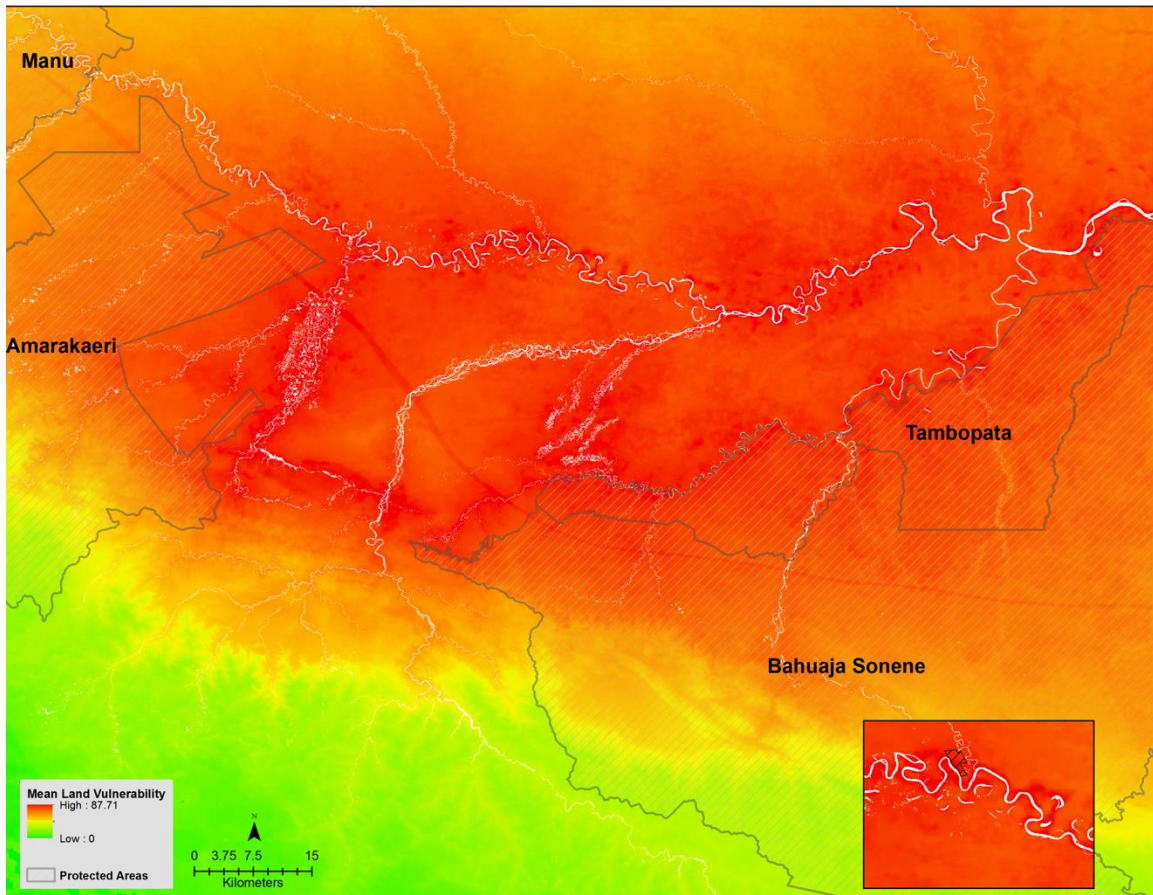


Figure 9 Mean land vulnerability to Hg pollution in the Madre de Dios Region of Peru. Protected areas outlined in black. Los Amigos Conservation Concession shown in insert.

Figure 10 shows the standard deviation of vulnerability from the five ORness values used in this study, indicating the degree to which vulnerability is sensitive to ORness value.

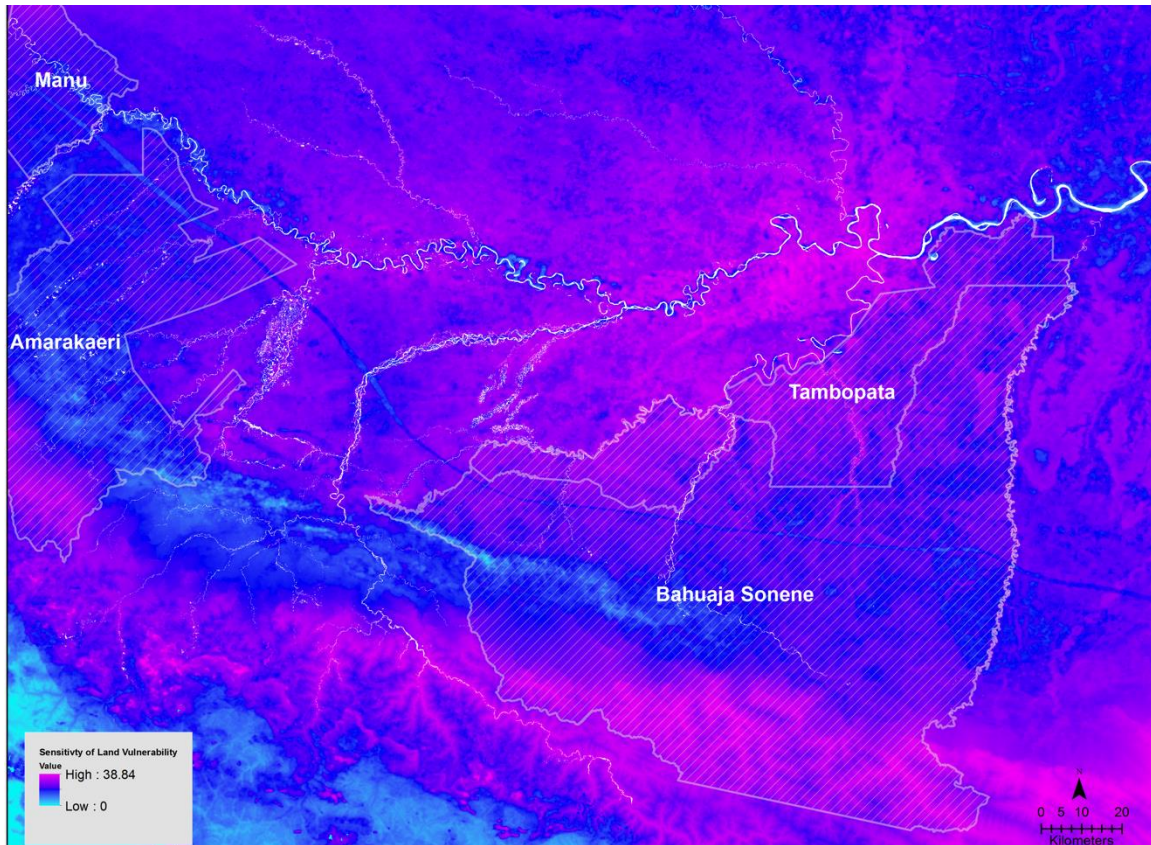


Figure 10 Sensitivity of land vulnerability model to ORness values. Protected areas outlined in white.

The complete range of vulnerability outputs for each ORness value is shown in Figure 11.



Figure 11 Range of river vulnerability dependent on ORness value ORness values increase from left to right. Vulnerability increases from green to red.

Riverine area vulnerability on average is very high along the Colorado River, with vulnerability scores 70 or higher (Fig 12). Portions of the Madre de Dios and Tambopata rivers also have high vulnerability as does the Malinowski River (Fig 12).



Figure 12 Mean river vulnerability to Hg pollution in Madre de Dios, Peru.

As expected, river vulnerability is also sensitive to ORness value as indicated by standard deviations (Figure 13).

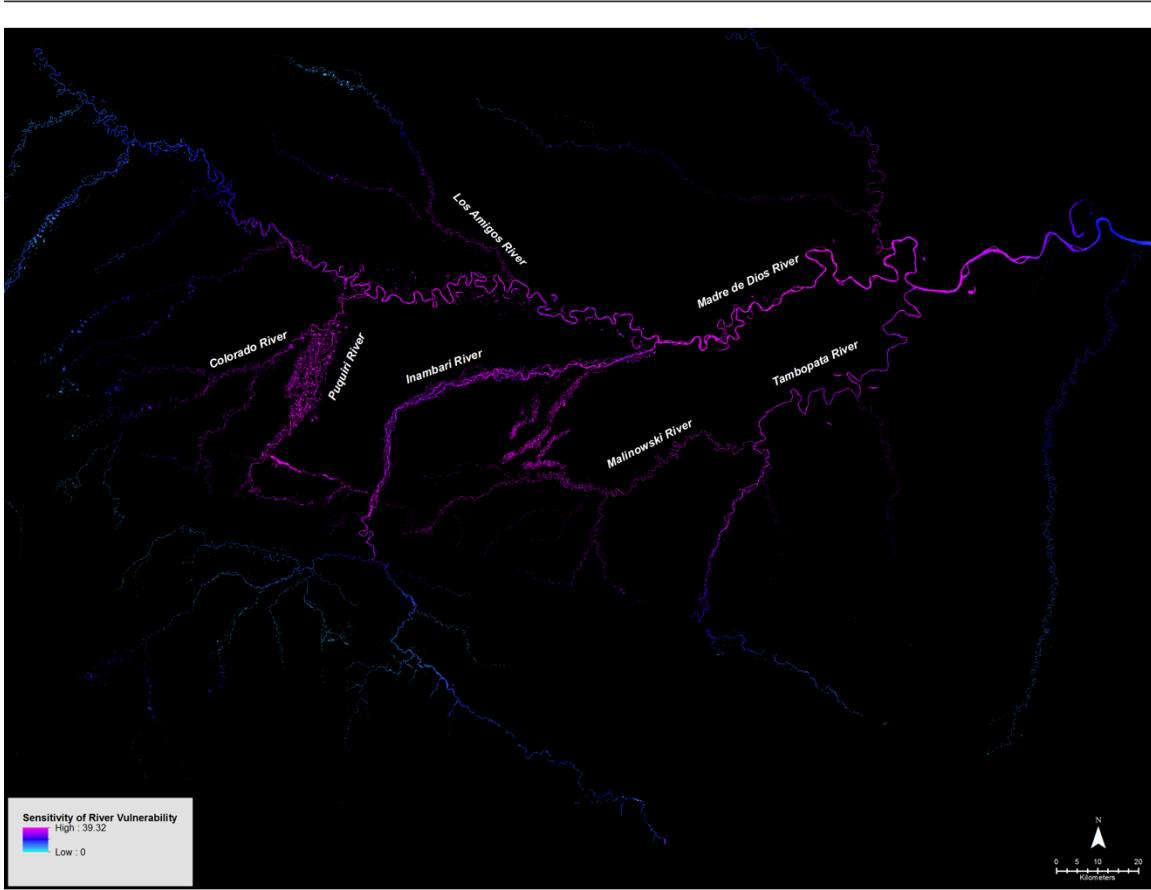


Figure 13 Sensitivity of river vulnerability model to ORness values

Mercury pollution and amphibian biodiversity

Amphibian biodiversity measured as species richness, increases as one moves from the Andes to the Amazon region (Fig 4). The distribution of each pixel's richness or irreplaceability versus its vulnerability is shown in Figure 14. Areas of high priority were identified as those with richness greater than 80 and vulnerability greater than 70 and are shown in Figure 15.

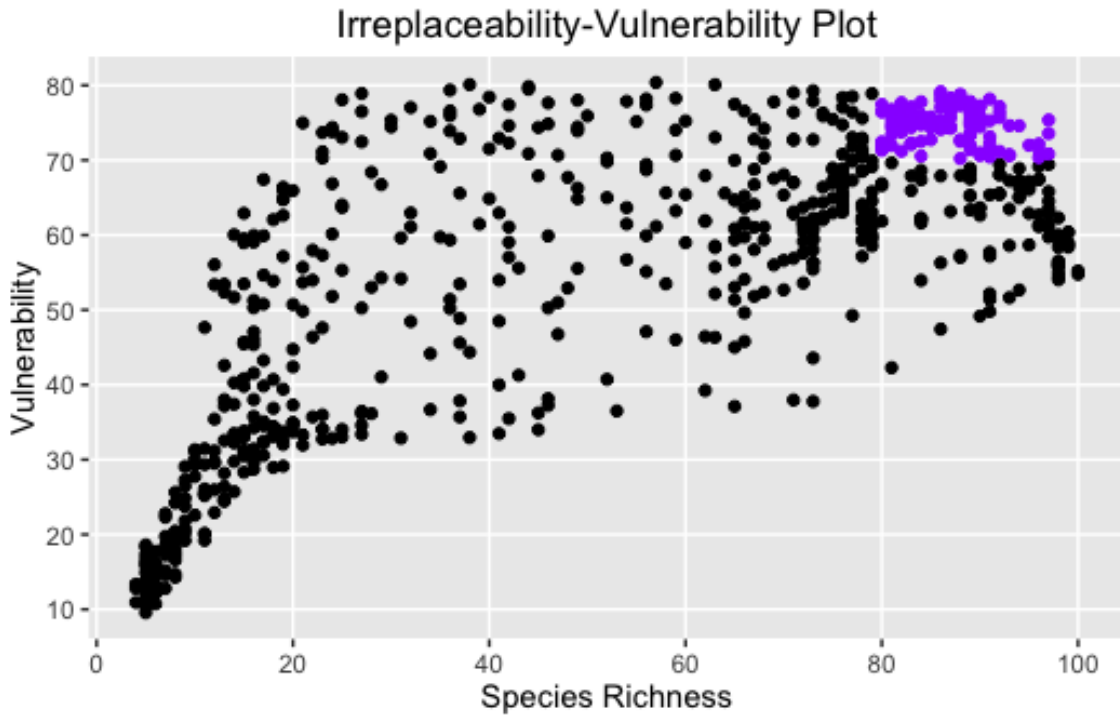


Figure 14 Irreplaceability-Vulnerability Analysis of Each 10km Pixel in Study Area.

Of the 10,700 km² area determined to be of high conservation priority (Fig 15), 8,292 km² or 75% are unprotected. High priority areas can be found along a portion of the Madre de Dios River as well as along the Tambopata River (Fig 15). Inside Tambopata National Reserve, 1888 km² of land are at the upper limits of both species richness and vulnerability, amounting to almost 18% of high priority area. In Bahuaja Sonene, 522 km² are presently considered to have both high vulnerability and species richness.

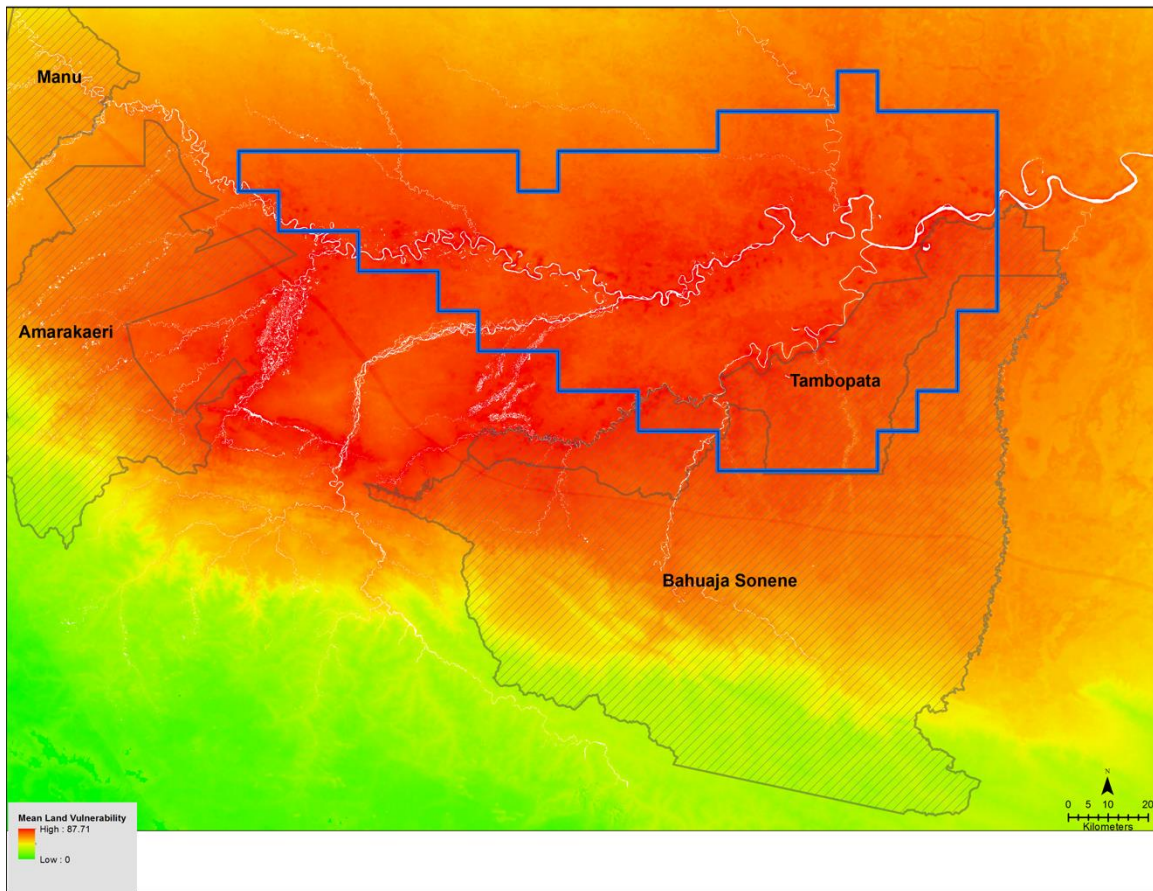


Figure 15 Average vulnerability to mercury with area of high priority for amphibian biodiversity conservation of (outlined in blue). Protected areas named and outlined in grey.

Discussion

We sought to determine how much the landscape of Madre de Dios has changed due to mining and to identify which areas are at greatest risk to Hg pollution. From 2001 to 2015, we determined that the study region experienced an increase in mining area of 115.97 km². Much of this increase was at the expense of forested areas. At an ORness level of 0.75, we found that 25,336 km² of land are vulnerable to Hg pollution. On average, we determined that 19,576 km² of land have a vulnerability of 70 or higher. We identified vulnerable area including land in Tambopata National Reserve, Bahuaja Sonene National Park, and Amarakaeri Communal Reserve (Fig 8). Areas of high vulnerability overlaps with areas where amphibian biodiversity is high. Rivers identified as having high vulnerability to Hg pollution include the Colorado River and portions of the Madre de Dios, Malinowski, and the Tambopata rivers.

An important contributor to Peru's economy, gold mining has significantly altered the landscape in Madre de Dios. Using iron oxide indices, true color composites, and tassal cap transformations measuring wetness and brightness, we were able to detect soils adjacent to known mining areas with spectral signatures separate from soil and sand from undisturbed and agricultural areas (see Appendix I). In using areas of agreement

between random forest and Mahalanobis classifications, land stated here as mining represents what is likely a conservative estimate. In-situ research and consultation with regional experts leads us to state with reasonable certainty that such area does represent soils that are heavily disturbed and contaminated with Hg from burning the amalgam of gold and Hg. Although on the ground accuracy assessment was low, this is likely because ground truth points were collected in accessible areas where development is extensive and on-going. Moreover, as visiting sites where mining was actively occurring proved unsafe, only edge areas were visited that are known to be more difficult to detect at 30m resolution. Most of the sites visited were either in the exploration stage of mining rather than actual extraction or highly heterogeneous. This represents a limitation of our validation, but one we do not believe affected our results, as maps were also verified with consultation with local experts and a combination of two classification methods was ultimately used to identify mining area.

Our estimates of changes in the landscape differ from Asner and colleagues' (2013) study which reports that Madre de Dios lost 500 km² of forest due to gold mining from 1999 to 2012 as well as with Elmes and colleagues' (2014) report of 650 km² of mining area. The exact study area for these studies does not perfectly align and different methods were used. Our study used the Random Forest classification to identify not areas deforested due to mining but areas of active mining whereas Asner and colleagues (2013) used the Carnegie Landsat Analysis System-lite (CLASlite) to identify mining extent. Thus, results presented in this paper represent a stricter classification of mining than Asner and colleagues' (2013) and do not take into consideration areas deforested for gold exploration but where mercury has not entered into the process. Elmes and colleagues (2014) used spectral unmixing and classification trees to identify soils thought typical of mining and classified more area as mining compared to this current study.

In many cases, we identified mining that is adjacent to protected areas (Fig 7). ASGM activity currently extends to the northwestern border of Tambopata National Reserve and appears to have crossed into the reserve itself, in agreement with maps produced by the Monitoring of the Andean Amazon Project (Finer et al., 2015; 2016). ASGM activity is also close to Amarakaeri Communal Reserve.

Along the Madre de Dios River, between the city of Puerto Maldonado and where the Inambari River joins the Madre de Dios, vulnerability to Hg pollution is high. Hg is likely transported along this portion of the Madre de Dios (MdD) from the Guacamayo mining area (Figure 1), where a substantial amount of ASGM activity occurs, as well as from pockets of ASGM activity occurring along the MdD itself. This area is largely unprotected except for ecotourism concessions to the west of the Inambari and the ecotourism concession Tiburcio Huacho.

The extent of area modeled as vulnerable to Hg pollution depends on the ORness level chosen (Figs 9 & 11). On average, 19,576km² of land have a vulnerability of 70 or higher,

but this area varies between 0.08 and 61,653 km² depending on the level of risk considered in the aggregation. At higher ORness levels, extends into protected areas and overlaps with portions of the study site with very high amphibian biodiversity.

Amphibians can be exposed to environmental pollutants such as MeHg in multiple ways: through water movement across the egg capsule, through their food, and through their permeable skin layer, which acts as a respiratory surface, as larvae, tadpoles, and adults (Linder et al., 2010). Increased or expanded protection may be necessary, as areas of high vulnerability exist outside protected areas and considering that Hg is transported from point sources in the air and settling on land or on water.

Additionally, amphibians are often considered the “sentinels” of change (Sparling et al., 2001; Kiesecker et al., 2004), and studying populations vulnerable to Hg pollution may give us an early warning system before the larger ecosystem is substantially threatened by Hg pollution.

The vulnerability models presented in this paper suggest that Hg pollution is likely threatening a considerable amount of Madre de Dios’s unmatched biodiversity. The largest mining activity on the landscape may not be the area most worthy of attention, as the Huepetuhe and Guacamayo mining areas are both found in locations where amphibian biodiversity is of moderate levels. Areas identified as high priority based on our methods includes areas where amphibian richness overlaps with high Hg vulnerability, and coincides with areas with smaller ASGM activities. Ten thousand, seven hundred square kilometers of land are classified as high conservation priority based on a combination of high vulnerability and high species richness. Of this, 1888.19 km² overlap with Tambopata National Reserve (Fig 13). Tambopata National reserve is not only a biodiversity hotspot but, is also a popular tourist site and includes the Tambopata Research Station.

Yet, areas outside the high priority zone indicated should not be disregarded, as our methods did not consider species’ population size, rates of decline, and existing threats. Areas modeled as having greater vulnerability should be investigated further to determine which, if any, populations of amphibians may be at risk, Further work should investigate other relevant threats and factors such as the health and red list status of amphibians within the area, and the feasibility of protecting such land. Areas determined to be of high priority should only be treated as such if the support of local actors is secured and the broader context of future ASGM mining activities and legislation is considered. This model should be used to determine future conservation actions holistically, with the input of local stakeholders and support from regional authorities.

In summary, our work suggests Hg pollution from ASGM is potentially threatening amphibian biodiversity in Madre de Dios, particularly in unprotected areas. ASGM activity has increased throughout the study area and vulnerability extends into

Tambopata National Reserve threatening the very high amphibian biodiversity found north of the Madre de Dios River. ASGM mining also occurs close to Amarakaeri Communal Reserve, where amphibian biodiversity is lower.

The neurotoxic effects of Hg coupled with the current global decline and extinction of amphibian species (Stuart et al., 2004) makes identifying and protecting areas of amphibian biodiversity a worthy cause. Future mining concessions should consider existing vulnerability and areas of high amphibian biodiversity when possible. Formal protection for areas of high biodiversity north of the Madre de Dios River may also prove needed. Yet ASGM in Madre de Dios is largely unregulated and illegal, thus legalizing and formalizing existing mining efforts should be considered. This could ensure workers have the proper tools and training to protect themselves and the surrounding ecosystems from the harmful effects of Hg and would likely have a real impact for both the industry and the biodiversity currently threatened.

Works cited:

Alho, C. J. R. (2008). The value of biodiversity. *Brazilian Journal of Biology*, 68(4), 1115-1118.

Alvarez-Berrios, Nora, et al. "Impacts of small-scale gold mining on birds and anurans near the Tambopata Natural Reserve, Peru, assessed using passive acoustic monitoring." *Tropical Conversation Science*, 9.2 (2016): 832-851.

Alvarez-Berríos, N. L., & Aide, T. M. (2015). Global demand for gold is another threat for tropical forests. *Environmental Research Letters*, 10(1), 014006.

Amazon Conservation Association (2009) Fact Sheet: Illegal Gold Mining in Madre de Dios, Peru.

Andren, A. W., & Harriss, R. C. (1975). Observations on the association between mercury and organic matter dissolved in natural waters. *Geochimica et cosmochimica acta*, 39(9), 1253-1258.

Asner GP, Llactayo W, Tupayachi R, and Ruez Luna E. (2013) Elevated rates of gold mining in the Amazon revealed through high-resolution monitoring. *PNAS*, 110 (46): 18454-18459.

Azad Hossain, A. K. M., Jia, Y., & Chao, X. (2010, September). Development of remote sensing based index for estimating/mapping suspended sediment concentration in river and lake environments. In *Proceedings of 8th international symposium on ECOHYDRAULICS (ISE 2010)* (pp. 578-585).

Baeyens, W., Leermakers, M., Papina, T., Saprykin, A., Brion, N., Noyen, J., ... & Goeyens, L. (2003). Bioconcentration and biomagnification of mercury and methylmercury in

- North Sea and Scheldt estuary fish. *Archives of Environmental Contamination and Toxicology*, 45(4), 498-508.
- Bagdanavičiūtė, I., & Valiūnas, J. (2013). GIS-based land suitability analysis integrating multi-criteria evaluation for the allocation of potential pollution sources. *Environmental earth sciences*, 68(6), 1797-1812.
- Baig, M. H. A., Zhang, L., Shuai, T., & Tong, Q. (2014). Derivation of a tasselled cap transformation based on Landsat 8 at-satellite reflectance. *Remote Sensing Letters*, 5(5), 423-431.
- Becker, C. G., Fonseca, C. R., Haddad, C. F. B., Batista, R. F., & Prado, P. I. (2007). Habitat split and the global decline of amphibians. *Science*, 318(5857), 1775-1777.
- Beijer, K., & Jernelov, A. (1979). Methylation of mercury in aquatic environments. In Nriagu, J. O. (Ed.), *The Biogeochemistry of Mercury in the Environment*. (pp. 203-208). Elsevier, North-Holland.
- Bengtsson, J., Jones, H., & Setälä, H. (1997). The value of biodiversity. *Trends in Ecology & Evolution*, 12(9), 334-336.
- Bergeron, C. M., Hopkins, W. A., Todd, B. D., Hepner, M. J., & Unrine, J. M. (2011). Interactive effects of maternal and dietary mercury exposure have latent and lethal consequences for amphibian larvae. *Environmental science & technology*, 45(8), 3781-3787.
- BirdLife International. (2016). Endemic Bird Area factsheet: South-east Peruvian lowlands. Downloaded from <http://www.birdlife.org> on 25/08/2016
- Breiman, L. (2001). Random forests. *Machine Learning*, 45(1), 5-32.
- Brown, J. H. (1995). *Macroecology*. University of Chicago Press. Chicago
- Burke, J. N., Bergeron, C. M., Todd, B. D., & Hopkins, W. A. (2010). Effects of mercury on behavior and performance of northern two-lined salamanders (*Eurycea bislineata*). *Environmental Pollution*, 158(12), 3546-3551.
- Carroll, R. W. H., Warwick, J. J., Heim, K. J., Bonzongo, J. C., Miller, J. R., & Lyons, W. B. (2000). Simulation of mercury transport and fate in the Carson River, Nevada. *Ecological Modelling*, 125(2), 255-278.
- Catenazzi A, Lehr E, & May RV (2013) The amphibians and reptiles of Manu National Park and its buffer zone, Amazon basin and eastern slopes of the Andes, Peru. *Biota Neotropica* 13(4): 269-283.

Chorley, R. J., & Haggett, P. (1965). Trend-surface mapping in geographical research. *Transactions of the Institute of British Geographers*, 47-67.

Cossa, D., Sanjuan, J., & Noel, J. (1994). Mercury transport in waters of the Strait of Dover. *Marine Pollution Bulletin*, 28(6), 385-388.

Craig, P. (1986). Organomercury compounds in the environment, in: *Organometallic Compounds in the Environment: Principles and Reactions* (pp. 65-110). Craig P.J., Ed., Longman, Harlow.

Diringer, S. E., Feingold, B. J., Ortiz, E. J., Gallis, J. A., Araújo-Flores, J. M., Berky, A., ... & Hsu-Kim, H. (2015). River transport of mercury from artisanal and small-scale gold mining and risks for dietary mercury exposure in Madre de Dios, Peru. *Environmental Science: Processes & Impacts*, 17(2), 478-487.

Douglas, I., & Lawson, N. (2002). Material flows due to mining and urbanization. RU Ayres, LW: Ayres, eds. *Handbook of Industrial Ecology*, 351-364.

Eastman, J. R. (2009). IDRISI Taiga guide to GIS and image processing. Clark Labs Clark University, Worcester, MA.

Ehrlich, P. R., & Ehrlich, A. H. (1992). The value of biodiversity. *Ambio* (Sweden).

Eisler, R., & Wiemeyer, S. N. (2004). Cyanide hazards to plants and animals from gold mining and related water issues. In *Reviews of Environmental Contamination and Toxicology* (pp. 21-54). Springer New York.

Elmes A, Yarlequé Ipanaqué JG, Rogan J, Cuba N, & Bebbington A (2014) Mapping licit and illicit mining activity in the Madre de Dios region of Peru. *Remote Sensing Letters*, 5(10): 882-891.

Environmental Protection Agency. (1996). U. S. *Method1669: Sampling Ambient Water for Trace Metals at EPA Water Quality Criteria Levels*. EPA-821-R-96-011.

Fagerström, T., & Jernelöv, A. (1972). Some aspects of the quantitative ecology of mercury. *Water Research*, 6(10), 1193-1202.

Finer, M., Novoa, S., Olexy, T. (2016). Illegal Gold Mining Penetrates Deeper into Tambopata National Reserve. MAAP: 24. <http://maaproject.org/2016/tambopat2/>

Finer, M., Novoa, S., Snelgrove, C., & Peña, N. (2015.) Confirming an Illegal Gold Mining Invasion of the Tambopata National Reserve (Madre de Dios, Peru) [High-Resolution View]. MAAP: 21 <http://maaproject.org/2015/tambopata/>

Fitzgerald, W. F., & Clarkson, T. W. (1991). Mercury and monomethylmercury: present and future concerns. *Environmental Health Perspectives*, 96, 159.

Gabr, S., Ghulam, A., & Kusky, T. (2010). Detecting areas of high-potential gold mineralization using ASTER data. *Ore Geology Reviews*, 38(1), 59-69.

Garmendia, E., Gamboa, G., Franco, J., Garmendia, J. M., Liria, P., & Olazabal, M. (2010). Social multi-criteria evaluation as a decision support tool for integrated coastal zone management. *Ocean & Coastal Management*, 53(7), 385-403.

Gaston, K. J. (1994). *What is rarity?* (pp. 1-21). Springer Netherlands.

George MW (2015) Mineral Commodity Summaries-Gold. (USGeological Survey, Reston, VA), 66-67.

Ghimire, B., Rogan, J., & Miller, J. (2010). Contextual land-cover classification: incorporating spatial dependence in land-cover classification models using random forests and the Getis statistic. *Remote Sensing Letters*, 1(1), 45-54.

Huang, C., Wylie, B., Yang, L., Homer, C., & Zylstra, G. (2002). Derivation of a tasselled cap transformation based on Landsat 7 at-satellite reflectance. *International Journal of Remote Sensing*, 23(8), 1741-1748.

Hengl, T., de Jesus, J. M., Heuvelink, G. B., Gonzalez, M. R., Kilibarda, M., Blagotić, A., ... & Guevara, M. A. (2017). SoilGrids250m: Global gridded soil information based on machine learning. *PloS one*, 12(2), e0169748.

Hines, M. E., Horvat, M., Faganeli, J., Bonzongo, J. C. J., Barkay, T., Major, E. B., ... & Lyons, W. B. (2000). Mercury biogeochemistry in the Idrija River, Slovenia, from above the mine into the Gulf of Trieste. *Environmental Research*, 83(2), 129-139.

Hopkins WA, Rowe CL (2010). Interdisciplinary and Hierarchical Approaches for Studying the Effects of Metals and Metalloids on Amphibians. In Sparling, D. W., Linder, G., Bishop, C. A., & Krest, S. (Eds.), *Ecotoxicology of Amphibians and Reptiles*. (pp. 325-336). CRC Press.

Horvat, M., Nolde, N., Fajon, V., Jereb, V., Logar, M., Lojen, S., ... & Drobne, D. (2003). Total mercury, methylmercury and selenium in mercury polluted areas in the province Guizhou, China. *Science of the Total Environment*, 304(1), 231-256.

Instituto de Investigaciones de la Amazonia Peruana y El Ministerio del Ambiente. Minería Aurífera en Madre de Dios Y Contaminación con Mercurio: Una bomba de tiempo. 2011.

Jensen, S., & Jernelöv, A. (1969). Biological methylation of mercury in aquatic organisms. *Nature*, 223(5207), 753-754.

Kauth, R. J., & Thomas, G. S. (1976, January). The tasselled cap--a graphic description of the spectral-temporal development of agricultural crops as seen by Landsat. In *LARS Symposia* (p. 159).

Kheir, R. B., Shomar, B., Greve, M. B., & Greve, M. H. (2014). On the quantitative relationships between environmental parameters and heavy metals pollution in Mediterranean soils using GIS regression-trees: the case study of Lebanon. *Journal of Geochemical Exploration*, 147, 250-259.

Kiesecker, J. M., Belden, L. K., Shea, K., & Rubbo, M. J. (2004). Amphibian Decline and Emerging Disease: What can sick frogs teach us about new and resurgent diseases in human populations and other species of wildlife?. *American Scientist*, 138-147.

Kotsiantis, S., & Pintelas, P. (2004). Combining bagging and boosting. *International Journal of Computational Intelligence*, 1(4), 324-333.

Krawczynski R (2006) Succession of Collembola in the post-mining landscape of lower Lusatia. Ph.D. Thesis. Department of Ecology, Brandenburg University of Technology, Cottbus, Germany.

Liaw, A., and Wiener, M. (2002). Classification and Regression by randomForest. *R News* 2(3), 18--22.

Lippitt, C. D., Rogan, J., Toledano, J., Sangermano, F., Eastman, J. R., Mastro, V., & Sawyer, A. (2008). Incorporating anthropogenic variables into a species distribution model to map gypsy moth risk. *Ecological Modelling*, 210(3), 339-350.

Linder, G.H., Lehman, C.M., & Bidwell, J.R. (2010). Ecotoxicology of Amphibians and Reptiles in a Nutshell. In Sparling, D. W., Linder, G., Bishop, C. A., & Krest, S. (Eds.), *Ecotoxicology of Amphibians and Reptiles*. (pp. 69-203). CRC Press.

Linke, S., Pressey, R. L., Bailey, R. C., & Norris, R. H. (2007). Management options for river conservation planning: condition and conservation re-visited. *Freshwater Biology*, 52(5), 918-938.

Low P (2012) Artisanal and Small-Scale Mining in Peru: A Blessing or a Curse? (Peru Support Group, London)

Majer JD (2014) Mining and Biodiversity: Are They Compatible?. In *Resource Curse or Cure?* (pp. 195-205). Springer Berlin Heidelberg.

- Majer, J. D., & Beeston, G. (1996). The biodiversity integrity index: an illustration using ants in Western Australia. *Conservation Biology*, 10(1), 65-73.
- Malczewski, J., Chapman, T., Flegel, C., Walters, D., Shrubsole, D., & Healy, M. A. (2003). GIS-multicriteria evaluation with ordered weighted averaging (OWA): case study of developing watershed management strategies. *Environment and Planning A*, 35(10), 1769-1784.
- Margules, C. R., & Pressey, R. L. (2000). Systematic conservation planning. *Nature*, 405(6783), 243-253.
- Mason, R. P., Fitzgerald, W. F., Hurley, J., Hanson, A. K., Donaghay, P. L., & Sieburth, J. M. (1993). Mercury biogeochemical cycling in a stratified estuary. *Limnology and Oceanography*, 38(6), 1227-1241.
- Mason, R. P., & Benoit, J. M. (2003). Organomercury compounds in the environment. *Organometallic compounds in the environment*. Wiley, 57-99
- Mason, R. P., Heyes, D., & Sveinsdottir, A. (2006). Methylmercury concentrations in fish from tidal waters of the Chesapeake Bay. *Archives of Environmental Contamination and Toxicology*, 51(3), 425-437.
- McMahon, G. (Ed.). (1999). *An environmental study of artisanal, small, and medium mining in Bolivia, Chile, and Peru* (Vol. 23). World Bank Publications.
- Naeem, S., Thompson, L. J., Lawler, S. P., Lawton, J. H., & Woodfin, R. M. (1994). Declining biodiversity can alter the performance of ecosystems. *Nature*, 368(6473), 734-737.
- Noss, R. F., Carroll, C., Vance-Borland, K., & Wuerthner, G. (2002). A multicriteria assessment of the irreplaceability and vulnerability of sites in the Greater Yellowstone Ecosystem. *Conservation Biology*, 16(4), 895-908.
- Pal, M. (2005). Random forest classifier for remote sensing classification. *International Journal of Remote Sensing*, 26(1), 217-222.
- Peres, C. A. (2001). Synergistic effects of subsistence hunting and habitat fragmentation on Amazonian forest vertebrates. *Conservation Biology*, 15(6), 1490-1505.
- Phua, M. H., & Minowa, M. (2005). A GIS-based multi-criteria decision making approach to forest conservation planning at a landscape scale: a case study in the Kinabalu Area, Sabah, Malaysia. *Landscape and Urban Planning*, 71(2), 207-222.

- Pimm, S. L., Jones, H. L., & Diamond, J. (1988). On the risk of extinction. *American Naturalist*, 757-785.
- Pour, A. B., & Hashim, M. (2015). Integration of Satellite Remote Sensing Data for Gold Prospecting in Tropical Regions. Paper presented at the 2015 Asian Conference on Remote Sensing in Manila, Philippines.
- Riscassi, A. L., Hokanson, K. J., & Scanlon, T. M. (2011). Streamwater particulate mercury and suspended sediment dynamics in a forested headwater catchment. *Water, Air, & Soil Pollution*, 220(1-4), 23-36.
- Saaty, T. L. (1977). A scaling method for priorities in hierarchical structures. *Journal of mathematical psychology*, 15(3), 234-281.
- Saaty, R. W. (1987). The analytic hierarchy process—what it is and how it is used. *Mathematical Modelling*, 9(3), 161-176.
- Sangermano, F., Toledano, J., & Eastman, J. R. (2012). Land cover change in the Bolivian Amazon and its implications for REDD+ and endemic biodiversity. *Landscape Ecology*, 27(4), 571-584.
- Scullion, J. J., Vogt, K. A., Sienkiewicz, A., Gmur, S. J., & Trujillo, C. (2014). Assessing the influence of land-cover change and conflicting land-use authorizations on ecosystem conversion on the forest frontier of Madre de Dios, Peru. *Biological Conservation*, 171, 247-258.
- Shafiee, S., & Topal, E. (2010). An overview of global gold market and gold price forecasting. *Resources Policy*, 35(3), 178-189.
- Shrum P. (2009) Analysis of mercury and lead in birds of prey from gold-mining areas of the Peruvian Amazon. Master's Thesis. Clemson, SC USA: Clemson University. http://tigerprints.clemson.edu/all_theses/753
- Sparling, D. W., Fellers, G. M., & McConnell, L. L. (2001). Pesticides and amphibian population declines in California, USA. *Environmental Toxicology and Chemistry*, 20(7), 1591-1595.
- Stuart, S. N., Chanson, J. S., Cox, N. A., Young, B. E., Rodrigues, A. S., Fischman, D. L., & Waller, R. W. (2004). Status and trends of amphibian declines and extinctions worldwide. *Science*, 306(5702), 1783-1786.
- Swenson JJ, Carter CE, Domec J, Delgado CI. (2011) Gold Mining in the Peruvian Amazon: Global Prices, Deforestation, and Mercury Imports. *PLoS ONE* 6: e18875.

Terborgh J, et al. (2008) Tree recruitment in an empty forest. *Ecology* 89(6): 1757–1768.

Todd, B. D., Willson, J. D., Bergeron, C. M., & Hopkins, W. A. (2012). Do effects of mercury in larval amphibians persist after metamorphosis?. *Ecotoxicology*, 21(1), 87-95.

Ullrich, S. M., Tanton, T. W., & Abdrashitova, S. A. (2010). Mercury in the aquatic environment: a review of factors affecting methylation. *Critical Reviews in Environmental Science and Technology*, 31(3), 241-293.

United States Geological Survey. (2015.) Mineral Commodity Summaries-Gold.

Villegas BC, Weinberg R, Levin E & Hund K. (2012) Artisanal and small-scale mining in protected areas and critical ecosystems programme (ASM-PACE) (Cambridge, UK: Estelle Levin and WWF) (www.profor.info/sites/profor.info/files/docs/ASM_PACE-GlobalSolutions.pdf)

Vitousek PM, Mooney HA, Lubchenco J, Melillo JM (1997) Human domination of Earth's ecosystems. *Science* 277: 494–499.

Warner, T. A., & Campagna, D. J. (2013). *Remote Sensing with IDRISI (R) Taiga: A Beginner's Guide*. Geocarto International Centre.

Webb, J. K., Brook, B. W., & Shine, R. (2002). What makes a species vulnerable to extinction? Comparative life-history traits of two sympatric snakes. *Ecological Research*, 17(1), 59-67.

Whitmore, T. C. (1997). Tropical forest disturbance, disappearance, and species loss. *Tropical forest remnants: ecology, management, and conservation of fragmented communities*. University of Chicago Press, Chicago, 3-12.

Wood, L. J., & Dragicevic, S. (2007). GIS-based multicriteria evaluation and fuzzy sets to identify priority sites for marine protection. *Biodiversity and Conservation*, 16(9), 2539-2558.

Yager, R. R. (1988). On ordered weighted averaging aggregation operators in multicriteria decisionmaking. *IEEE Transactions on systems, Man, and Cybernetics*, 18(1), 183-190.

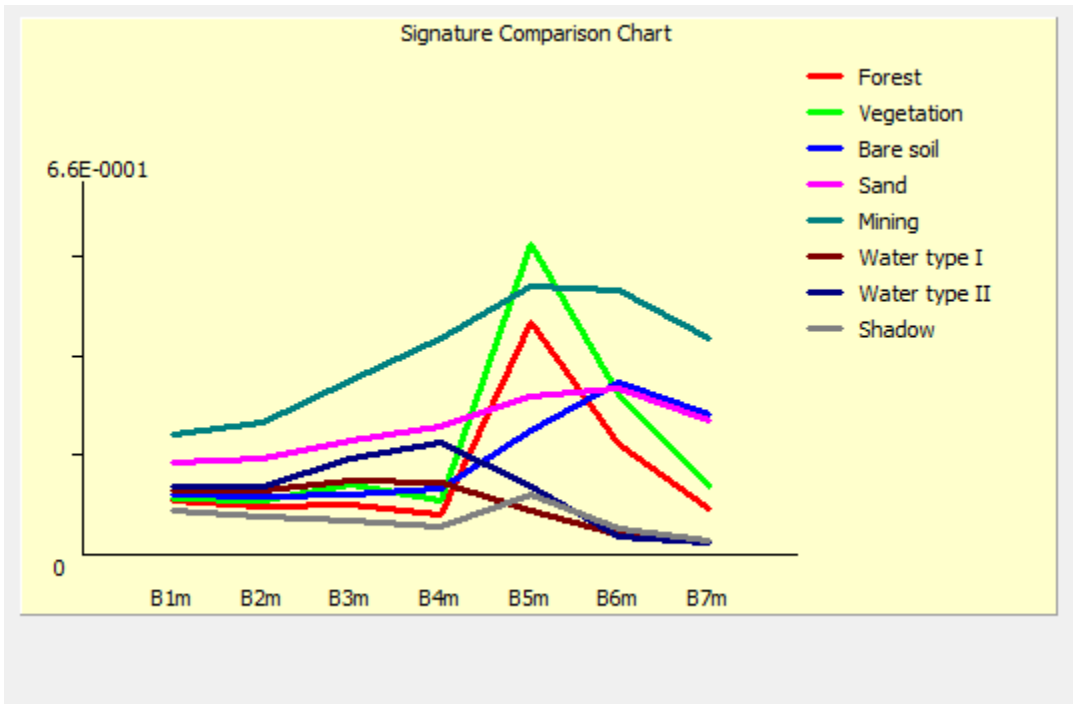
Žagar, D., Knap, A., Warwick, J. J., Rajar, R., Horvat, M., & Četina, M. (2006). Modelling of mercury transport and transformation processes in the Idrijca and Soča river system. *Science of the Total Environment*, 368(1), 149-163.

Zhang, H., Feng, X., Larssen, T., Shang, L., Vogt, R. D., Rothenberg, S. E., ... & Lin, Y. (2010). Fractionation, distribution and transport of mercury in rivers and tributaries around Wanshan Hg mining district, Guizhou province, southwestern China: Part 1—Total mercury. *Applied Geochemistry*, 25(5), 633-641.

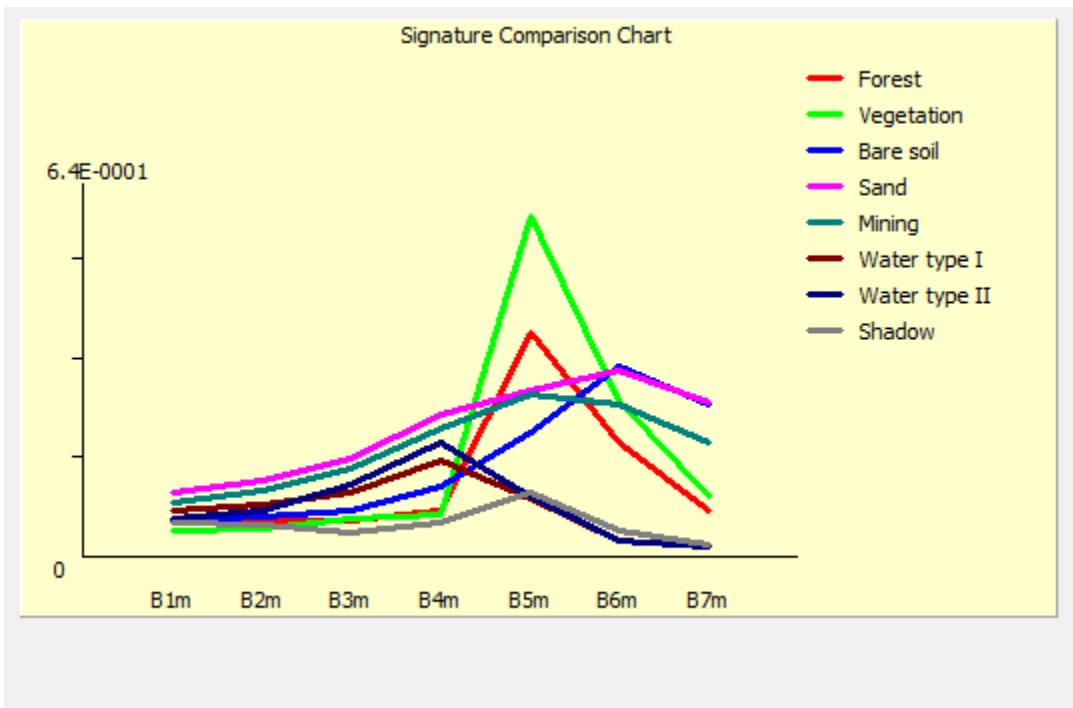
Appendices

Appendix I

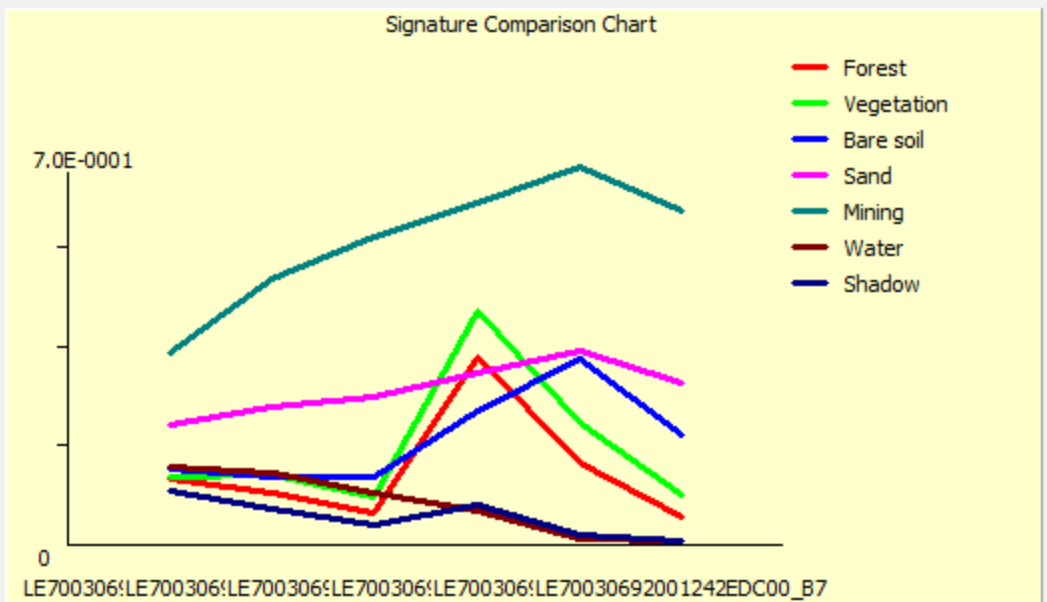
Spectral signatures of training sites for random forest



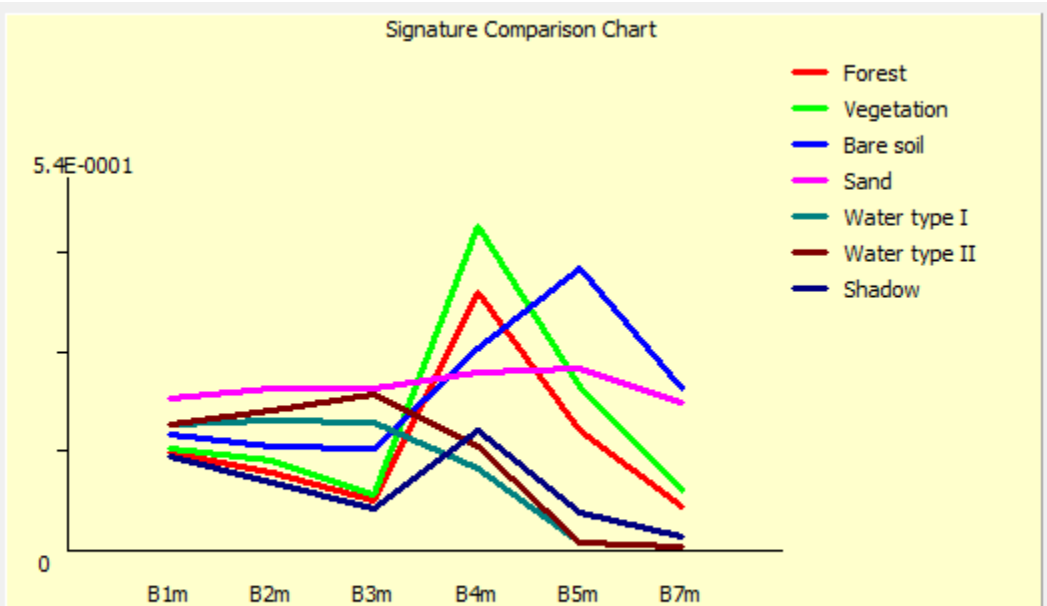
Spectral signatures for 2015 training sites for scene 3/69



Spectral signatures for 2015 training sites for scene 2/69



Spectral signatures for 2001 training sites for scene 3/69



Spectral signatures for 2001 training sites for scene 2/69

Appendix II

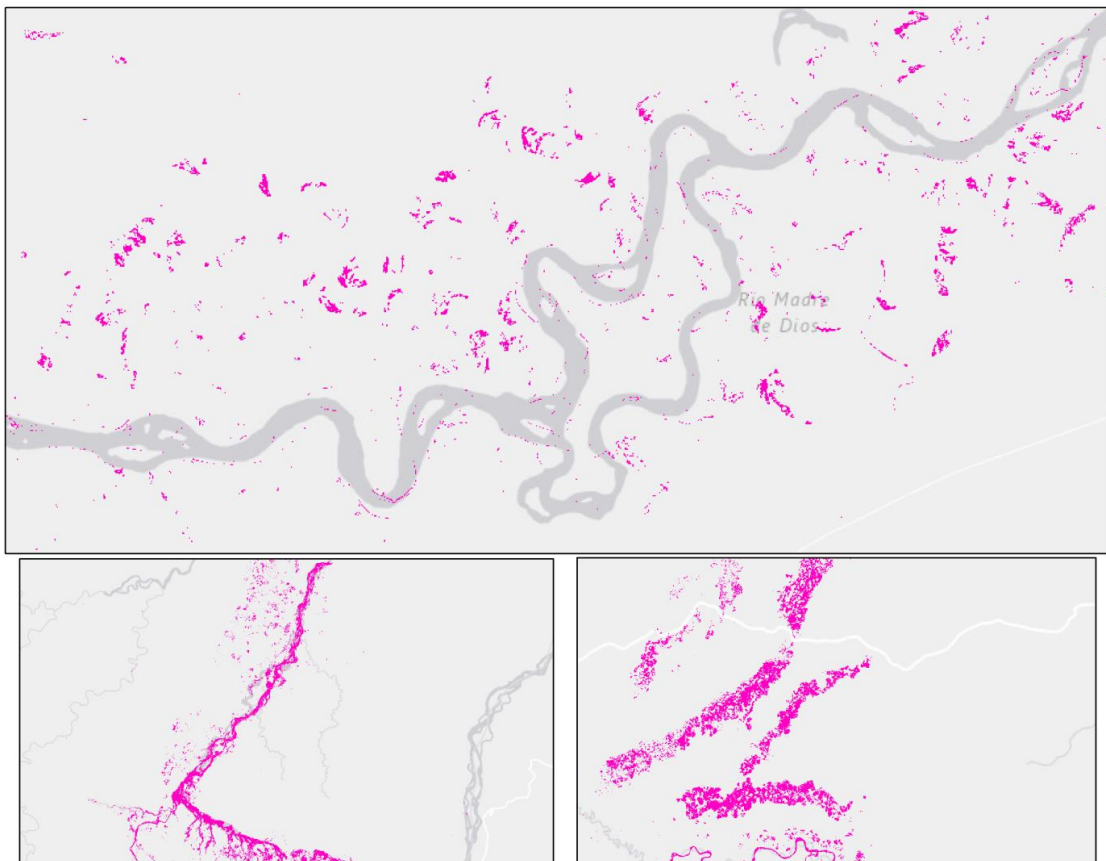
Landsat scenes used to create total suspended sediment index

Month, Day, and Year of Images Used for Index

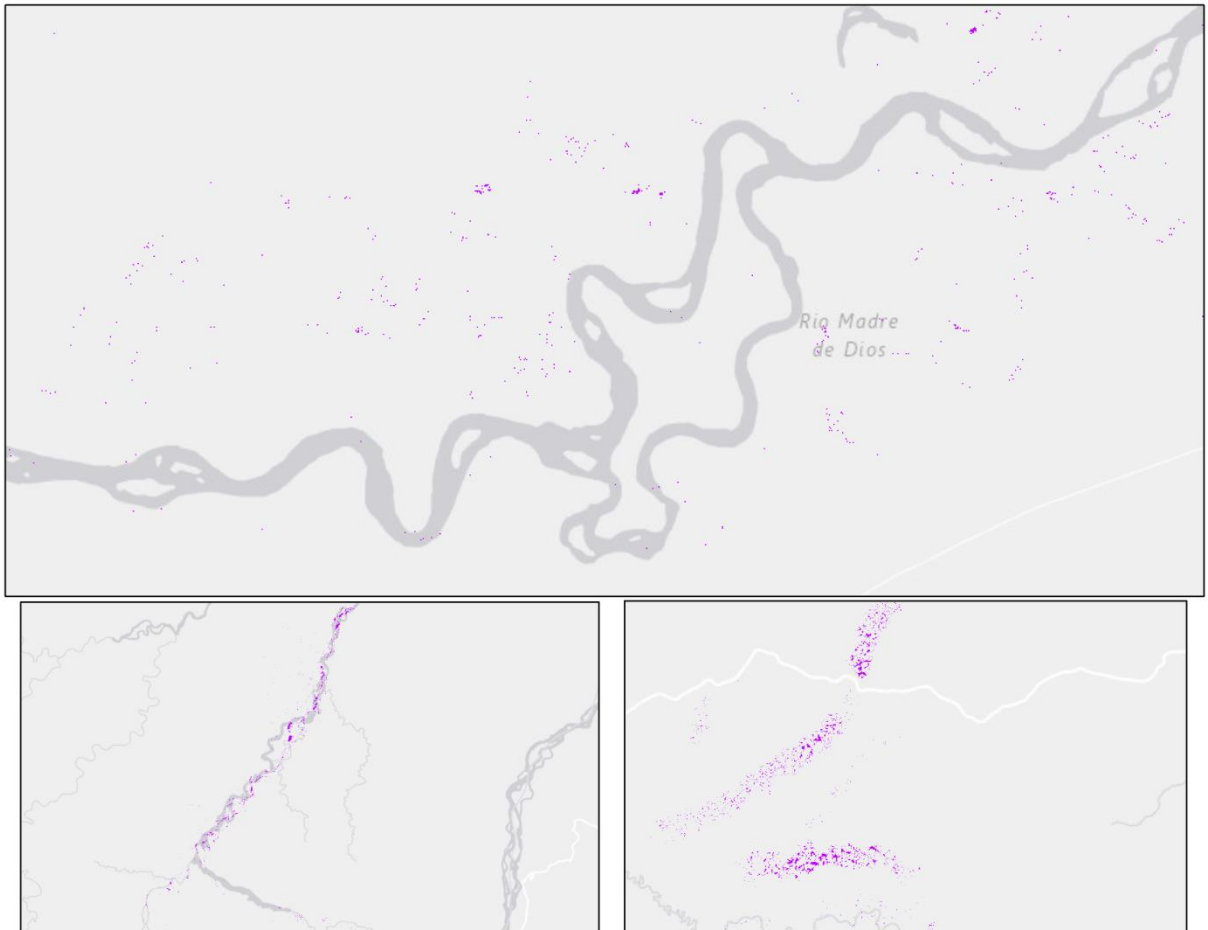
<i>Tile 3/69</i>	<i>Tile 2/69</i>
September 16, 2016	September 9, 2016
August 29, 2015	August 22, 2015
October 13, 2014	October 22, 2014
August 10, 2014	August 19, 2014
July 6, 2013	July 31, 2013
July 22, 2013	August 16, 2013

Appendix III

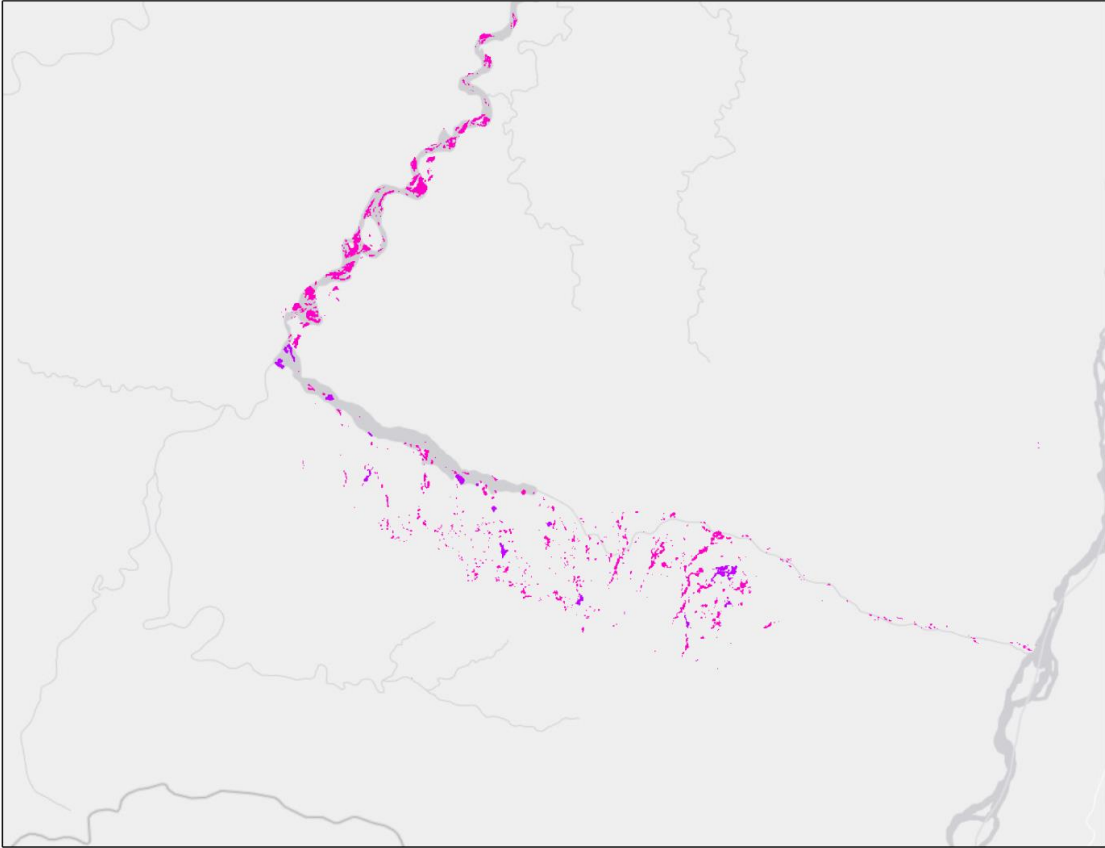
Mining area identified by random forest and Mahalanobis classification



Mining area identified using random forest classification for 2015 with 75% threshold



Mining area identified using Mahalanobis typicality classification for 2015 with 40% threshold



Mining area identified using random forest and Mahalanobis classifications (in pink and purple respectively) for 2001 with thresholds of 75 and 40%